# Chapter 11
# Synthesis of II-VI Semiconductor Nanocrystals


**Ghenadii Korotcenkov and Igor A. Pronin**

## 11.1 Introduction

As is known, devices based on II-VI compounds can be manufactured using both thin-film and thick-film technologies. As a rule, thin-film technology is based on the principles of synthesis of semiconductor compounds directly on the surface of substrates during their deposition or transfer of a semiconductor compound formed by various methods from a source to a substrate. For this purpose, various technologies for the deposition of semiconductor compounds are used, such as thermal evaporation, sputtering, laser ablation, chemical deposition, chemical vapor phase deposition, electrochemical deposition, etc. These methods are described in Chap. 10 (Vol. 1). In this case, the parameters of the semiconductors in the formed films, such as the crystallite size, orientation, and morphology of the films, are determined by the conditions used to deposit these films. In the case of thick-film technology, we may have a completely different situation. For the manufacture of devices based on II-VI compounds using thick-film technologies, such as screen printing (Fig. 11.1), spin coating (Fig. 11.2a), inkjet printing, drop, spray (Fig. 11.2b), and dip coating (Fig. 11.2c), etc., it is possible to use already synthesized powders of these compounds. In this case, the structural parameters of semiconductor-forming films will not depend on the conditions of film formation but will be determined by the conditions of synthesis of their powders. For the formation of films, one can also use pre-synthesized sol and gel of II-VI semiconductors and carry out their crystallization on the surface of the substrates. Each of these methods has its own advantages and disadvantages. They are discussed in detail in [100, 101].

G. Korotcenkov (✉)
Department of Physics and Engineering, Moldova State University, Chisinau, Moldova

I. A. Pronin
Department of Nano- and Microelectronics, Penza State University, Penza, Russia



G. Korotcenkov (ed.), *Handbook of II-VI Semiconductor-Based Sensors and Radiation Detectors*, https://doi.org/10.1007/978-3-031-19531-0_11

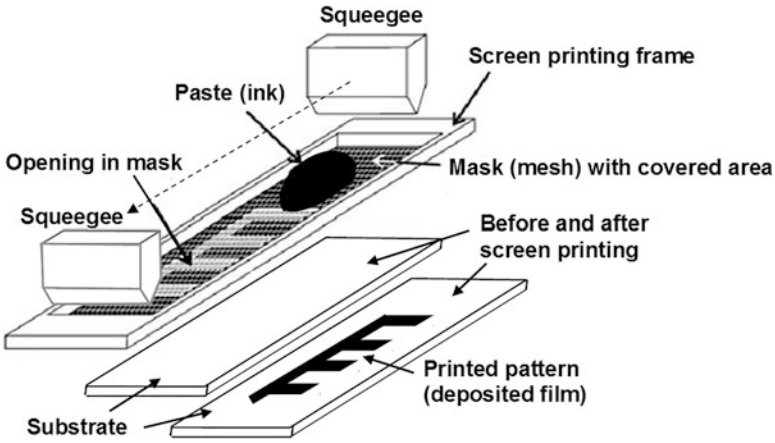


**Fig. 11.1** Manufacture of thick-film structures by screen printing. (Idea from Ref. [56])

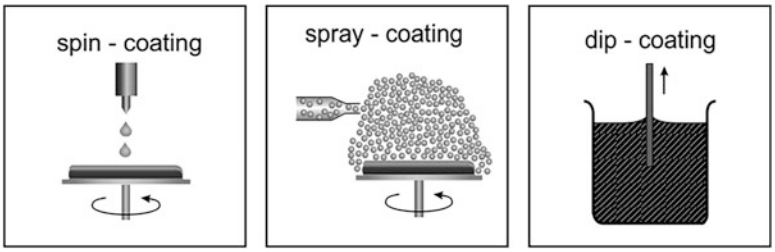


**Fig. 11.2** Illustration of the commonly used coating techniques. (Reprinted with permission from Ref. [170]. Copyright 2004: Elsevier)

As we indicated earlier, the technologies for film deposition of II-VI compounds are already described earlier in Chap. 10. Therefore, in this chapter, we focus on the consideration of methods for the synthesis of nanocrystallites (powders) of II-VI compounds used in thick-film technology.

## 11.2 Mechanochemical Method

Grinding is one of the oldest methods for the synthesis of fine particles from solid precursors. In this method, mechanical energy is used to break the atomic bonds of the precursor and form new materials [146]. The mechanochemical method is a combination of mechanical and chemical phenomena on a solid material at the nanoscale. This method makes extensive use of the ball mill, in which a powder mixture is placed in a ball mill and subjected to a high-energy impact from the balls. Mechanochemical processing is characterized by repeated welding, deformation,

and destruction of the mixture of reagents. Chemical reactions take place at nanometer-sized grain boundaries, which are continuously regenerated during the grinding process [98]. Therefore, chemical reactions that normally require high temperatures due to separation of reaction phases into product phases can take place at low temperatures in a ball mill without the need for external heating [215]. In addition, it is very easy to introduce impurities in this method with less effort, high uniformity, and high yield [88].

The rotation speed of the balls collision determines the efficiency of the grinding mechanism. The grinding capability also depends on the number of balls and ball diameter, as the ball diameter is inversely proportional to the frequency of the balls collisions. The structure, shape, and morphology of nanomaterials strongly depend on the parameters of bill milling strategy. For example, it was found that the energy of the mill is not critical for the final microstructure, but the kinetics of the process depends on the energy. The time required to reach the same microstructure can be several orders of magnitude longer in low-energy mills than in high-energy mills. It has also been suggested that the total strain introduced by milling is responsible for determining the nanocrystalline grain size [97]. With an appropriate choice of milling parameters and growth conditions, it is possible to produce nanomaterials in the form of diverse shapes like particles, rods, cubes, fibers, etc.

During this high-energy ball milling process, there is a choice to add a surfactant. Without a surfactant, the aggregation process takes place because of high surface energy of the particles, which results in the formation of larger NPs during mechanical grinding. If the surfactant is added, then the surfactant molecules form an organic layer on the surface of particles. The adsorption of these molecules lowers the surface energy of particles, and consequently no agglomeration takes place and NPs are produced with smaller size range and desired surface properties.

Examples of the implementation of the mechanochemical synthesis method as applied to II-VI compounds are given in Table 11.1. It can be seen that the simplest precursors such as Zn, Cd, Te, S, and Se powders can be used to synthesize nanoparticles of II-VI compounds.

It was established that the mechanochemical method makes it possible to synthesize nanoparticles of II-VI compounds of small size. For example, Godočíková et al. [52] reported that using this method they synthesized CdS NPs with average size of 9 nm. According to Kristl et al. [103], their CdS NPs had the size of ~8 nm.

Tsuzuki and McCormick [198] studied CdS nanoparticles synthesized by mechanochemical process and found the presence of mixed cubic and hexagonal phases in CdS NPs, prepared by using balls of diameter of 12.6 mm. However, when the ball size was reduced to 4.8 mm, the samples turned out to be completely in the cubic crystal structure. Furthermore, it was found that particle size of the product decreased in direct proportion to the size of milling balls. This means that this method appears to be an appropriate route for optimizing crystalline structure by suitable selection of milling conditions.

Another important process parameter is the milling time. In particular, Tan et al. [193] studied the process of CdS NCs synthesis with capping agent trioctylphosphine oxide/trioctylphosphine/nitric acid (TOPO/TOP/NA). They

**Table 11.1** Cd containing II-VI semiconductor nanomaterials prepared using different mechanochemical synthesis conditions

| II-VI | Precursors | Loading conditions of mills | Milling rate | Atmosphere | Ref. |
|---|---|---|---|---|---|
| CdS | Cd and S powders | 2–12 mm diameter | | Inert gas | [193] |
| | $Na_2S$, $CdCl_2$, and NaCl | 4.8–12.6 mm diameter | n/a | Inert gas | [198] |
| | Cadmium acetates and sodium sulfide | 50 balls of 10 mm diameter | 500 rpm | Argon | [11, 36] |
| | | 3 mm diameter | 350 rpm | Air | [197] |
| CdSe | Cd and Se powders | 2–12 mm diameter | n/a | Inert gas | [192] |
| CdTe | Cd and Te powders | 2–12 mm diameter | n/a | Inert gas | [194] |
| CdS, CdSe, CdTe | Cd, S, Se, and Te powders | n/a | n/a | Air | [103] |

found that the CdS-related XRD peak was not detected during the first 30 min of milling, while milling for 10 h appeared to completely convert the element precursors into CdS NPs. Tolia et al. [197] obtained similar results. It was observed that phase transformation of CdS NPs takes place after 6 h milling time. In addition to structural changes, there is also a change in the size of nanoparticles. Tan et al. [194] reported that the size of CdTe NPs was decreased from 23 to 3.5 nm when milling time was increased from 4.5 to 50 h.

The top-down method, such as mechanochemical synthesis, is an inexpensive, well-established, and traditional method for obtaining large-scale nanomaterials [167]. Moreover, this method is applicable to almost all classes of materials. However, the synthesized nanomaterials are often irregular in shapes and have defects. As a result of mechanical milling, additional mechanical tensions appear in the material. The appearance of mechanical tensions and structural defects can be an important factor that influences properties of synthesized materials. Therefore, these factors should be taken into account when designing technology of device fabrication. These tensions are only removed by thermal treatment. Thus, an additional thermal treatment after mechanical milling may be required.

Contamination, long processing time, no control on particle morphology, agglomerates, and residual strain in the crystallized phase are other disadvantages of high-energy ball milling process. In fact, the contamination problem is often presented as a reason to dismiss this method, at least for some materials. If steel balls and containers are used, iron contamination becomes a problem. This is the most serious problem for the highly energetic mills, and it depends on the mechanical

behavior of the powder being milled as well as its chemical affinity for the milling media. Lower-energy mills result in much less, often negligible, iron contamination. Other milling media, such as tungsten carbide or ceramics, may be used, but contamination is also possible from such media [97]. Surfactants (process control agents) may also be used to minimize contamination.

## 11.3 Co-precipitation Methods

Co-precipitation from solution is one of the oldest methods for preparing metal–chalcogenides with good compositional control. This process involves dissolving a salt precursor, usually sulfates, nitrates, etc., in some appropriate medium to form a uniform solution containing ion clusters. In this method, a basic precursor's solution is prepared by dropwise mixing in solvents, such as de-ionized water, ethanol, methanol, and acidic solutions, to better control the pH value [231]. Then, at room temperature, these prepared solutions are mixed and stirred for hours to fully react.

Figure 11.3 shows a schematic representation of the mechanism proposed to explain the formation of uniform particles during co-precipitation synthesis. In a homogeneous precipitation, a short single burst of nucleation occurs when the concentration of the constituent species reaches critical supersaturation. The nucleation continues until the monomer concentration drops below a critical threshold value, resulting in the quenching of the nucleation process. The nuclei thus obtained are then allowed to grow uniformly by diffusion of the solutes from the solution onto

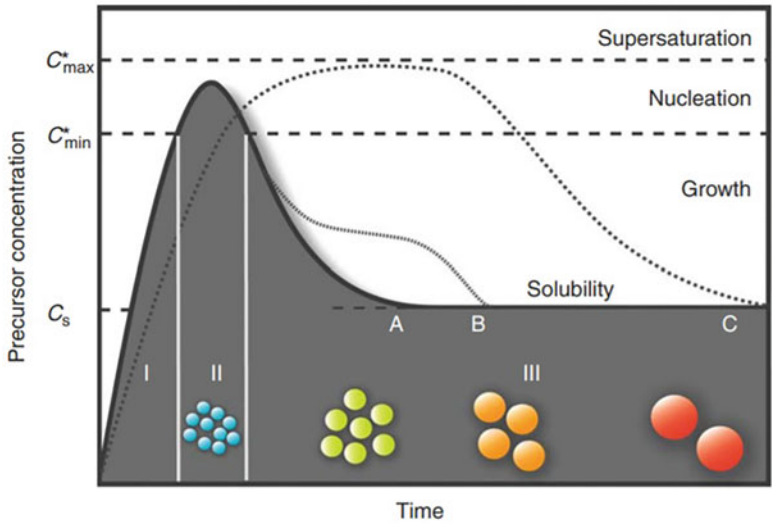


**Fig. 11.3** Mechanisms of monodisperse colloid formation. (Reprinted with permission from Ref. [232]. Copyright 2011: Elsevier)

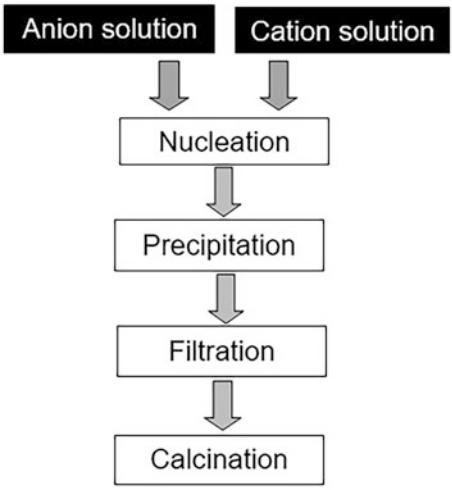


**Fig. 11.4** Schematic presentation of co-precipitation method

their surface until the final size is reached. To achieve monodispersity, it is necessary to separate these two stages and avoid nucleation during the growth time. This is the classical model first proposed by Lamer and Dinegar [108] to explain the mechanism of formation of sulfur colloids.

Thus, the precipitation includes several processes that occur simultaneously including initial nucleation (formation of small crystallites), growth (aggregation), coarsening, and agglomeration. In chemical precipitation, the reactants precipitate as precursors after the completion of the reaction due to their low solubility. The solubility of precursors depends on the pH value. Metal salts often require an alkaline/weak acidic environment for this process, so a well-organized pH is needed for the reaction. Chemical composition is an essential feature influencing the structures and properties of nanomaterials. Therefore, it is necessary to accurately organize the stoichiometric ratio of precursors. Solution pH, mixing rates, temperature, and concentration of precursors have to be also controlled to obtain satisfactory results [161]. For example, the addition of NaOH to the Se precursor during the synthesis of CdSe NPs accelerated nucleation and increased the concentration of CdSe QDs [46]. According to Lee et al. [122], with an increase in the content of $CdCl_2$ in the solution for synthesis of CdS NPs, a transformation of the crystalline phase from cubic to hexagonal is observed.

Finally, the precipitated product with low solubility in the solvent is separated from the liquid by filtration. Different stages involved in the synthesis of nanomaterials using co-precipitation are presented in Fig. 11.4. As is seen, the calcination at elevated temperature for several hours is the final operation in the co-precipitation method. Thus, co-precipitation comprises two main steps: (1) a chemical synthesis in the liquid phase that determines the chemical composition and (2) a thermal treatment that determines the crystal structure and morphology [134]. However, in the case of II-VI compounds, the annealing temperature usually

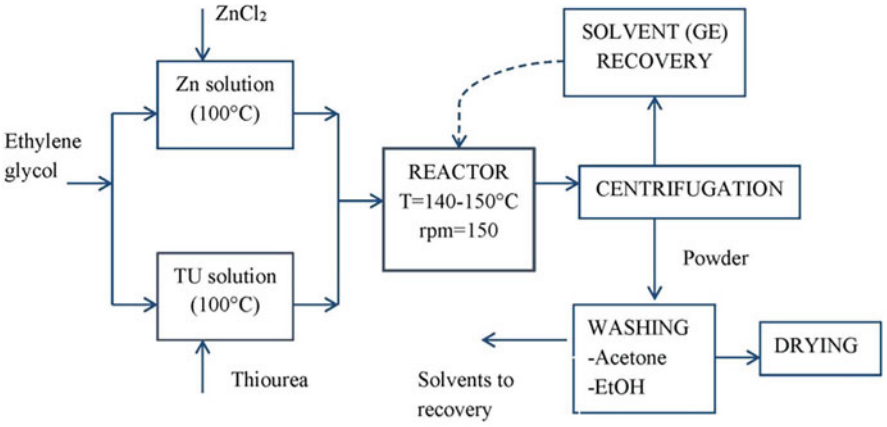


**Fig. 11.5** The schematic representation of the ZnS nanopowder synthesis. (Reprinted from Ref. [210]. Published 2021 by MDPI as open access)

does not exceed 130–200 °C, and the annealing itself is carried out in an inert or reducing atmosphere. In some cases, no heat treatment is used at all.

The experiment has shown that the co-precipitation method applied to II-VI compounds makes it possible to synthesize stoichiometric nanocrystals with sizes ranging from a few nm to 80 nm. For example, Rao et al. [159] synthesized very well-structured CdS nanoparticles with a size of 13 nm. Devi et al. [31] using $CdCl_2$, $Na_2S$, tetrabutylammonium bromide, and water as a solvent prepared stoichiometric CdS NPs with cubic structure and their size varying in the range of 15–80 nm. Raj and Rajendran [158] by reaction of cadmium acetate and sodium sulfide in aqueous environment synthesized CdS NPs with an average particle size of 7 nm. The temperature of the solution during the synthesis, depending on the solvent used, can vary within 40–160 °C. As a rule, with increasing temperature, the size of nanocrystallites formed in the process of co-precipitation increases [46]. Temperature conditions in relation to synthesis of ZnS NPs in ethylene glycol (EG)-based solution are given in Fig. 11.5.

Nanocrystals of other II-VI compounds, such as CdTe [53], CdSe [46], ZnS [81], ZnTe [139], and various heterostructures such as CdTe/CdS [204] have also been successfully synthesized using the co-precipitation method. For example, Mntungwa et al. [139] for the synthesis of ZnTe NPs suggested using the following reactions:

$$2\,\mathrm{Te} + 4\,\mathrm{NaBH_4} + 7\,\mathrm{H_2O} \rightarrow 2\,\mathrm{NaHTe} + \mathrm{Na_2B_4O_7} + 14\,\mathrm{H_2}\uparrow \quad (11.1)$$

$$\mathrm{NaHTe} + \mathrm{ZnCl_2} \rightarrow \mathrm{ZnTe} + \mathrm{NaCl} + \mathrm{HCl} \quad (11.2)$$

$$2\,\mathrm{NaHTe} + 2\,\mathrm{ZnSO_4} \cdot 7\mathrm{H_2O} \rightarrow 2\,\mathrm{ZnTe} + \mathrm{Na_2SO_4} + \mathrm{H_2SO_4} + 14\,\mathrm{H_2O} \quad (11.3)$$

$$\mathrm{NaHTe} + \mathrm{Zn(NO_3)_2} \cdot 6\mathrm{H_2O} \rightarrow \mathrm{ZnTe} + \mathrm{NaNO_3} + \mathrm{HNO_3} + 6\mathrm{H_2O} \quad (11.4)$$

Iranmanesh et al. [81] using zinc acetate ($Zn(Ace)_2{\cdot}2H_2O$) and sodium sulfide ($Na_2S$) and ethylenediaminetetraacetic acid (EDTA) as a stabilizer and capping agent synthesized ZnS nanocrystals with average particle size of 50 nm.

It is shown that the co-precipitation method also makes it possible to dope II-VI compounds. In particular, cerium-doped CdS NPs have been prepared by using co-precipitation technique [166]. The doping of Ce atom was carried out at concentrations of 1, 2, and 3 mol%. Both the doped and undoped NPs were found having wurtzite structure with particle size of 3 nm. The co-precipitation synthesis and characterization of Mn-doped CdS NPs have been reported by Gupta and Kripal [60]. The grown material had a wurtzite structure and a crystallite size of 2–4 nm. Elavarthi et al. [40] reported the preparation of pure and Cr-doped CdS NPs using chemical co-precipitation process. The doping at 3–5% Cr concentration appeared to change the structure of the NPs. Muruganandam et al. [142] carried out the preparation of polyvinylpyrrolidone (PVP)-capped CdS NPs and doping with Cu and Mn using chemical precipitation technique. Co-precipitation technique was also used to synthesize the Cr-doped CdSe NPs [127]. With increasing the chromium doping concentration, the lattice parameters showed a consistent decrease in such a way that for 4, 5, and 6% doping concentration, the size of NPs was 3.02, 2.48, and 2.11 nm, respectively.

The advantage of co-precipitation method is its low-cost and simple equipment, simple water-based reaction, flexibility, mild reaction conditions, comparatively low temperature, and size control. The composition control and purity of the resulting product are good. One disadvantage of this method is the difficulty to control the particle size and size distribution. In addition, this method is not suitable for the reactants, which have dissimilar solubility and precipitate rate. Different rates of precipitation of each individual compound may lead to microscopic inhomogeneity. Moreover, very often, fast (uncontrolled) precipitation takes place resulting in large particles. In addition, aggregates are generally formed, as with other solution techniques. Therefore, the use of surfactants is a common practice to prevent agglomeration, which also affects the particle size of the composites obtained by this technique [83].

## 11.4 The Sol–Gel Processing

Sol–gel techniques for the preparations of various materials have long been known and described in several books and reviews [28, 57]. A *sol* is a dispersion of colloidal solid particles (~0.01–1 μm) in a liquid in which only Brownian motion suspends the particles. In a *gel,* liquid and solid are dispersed within each other, presenting a solid network, containing liquid components. In this method, a liquid (sol) is chemically converted into gel state followed by condensation in the form of solid nanostructures.

It was established that through sol–gel process, homogeneous inorganic materials with desirable properties of hardness, optical transparency, chemical durability, tailored porosity, and thermal resistance can be produced at room temperatures [18, 76, 99, 115]. The surfactant-free process involves the simple wet chemical reaction based on hydrolysis of metal reactive precursors, usually metal chlorides, metal nitrates, and alkoxides in an alcoholic solution, and condensation, leading to formation of sol, which through the process of aging results in formation of an integrated network of metal hydroxide as gel. The gel is a polymer of three-dimensional skeleton surrounding interconnected pores. Different reactions can create the cross-linkages that result in the gelation of the solution [18, 28].

According to Brinker and Scherer [18], sol–gel polymerization occurs in three stages. First, the monomers are polymerized to form particles, followed by the growth of particles, and finally, the particles are linked into chains. Networks then extend throughout the liquid medium, thickening into a gel. The characteristics and properties of a sol–gel inorganic network are related to a number of factors that affect the rate of hydrolysis and condensation reactions: the pH level, the temperature and time of the reaction, the reagent concentrations, the nature and concentration of the catalyst, the $H_2O/M$ molar ratio (R), the aging temperature, and the drying time. Among these factors, the pH level, the nature and concentration of the catalyst, the $H_2O/M$ molar ratio (R), and the temperature were identified as the most important [18]. Although hydrolysis can occur without the addition of an external catalyst, it is more rapid and complete when a catalyst is employed. Mineral acids (HCl) and ammonia are used most often; however, other catalysts may be used as well, including acetic acid, KOH, amines, KF, HF, and $H_2O_2$.

Removal of the solvents and appropriate drying of the gel is an important step in the sol–gel process. When the sol is cast into a mold, a wet gel forms. With further drying, the gel is converted into dense particles. If the liquid in a wet gel is removed under a supercritical condition, a highly porous and extremely low-density material, called an aerogel, is obtained. Heat treatment of the gel is a final step that leads to the forming of ultrafine powders. Nanoparticles in the gel are often amorphous, and the thermal treatment imparts the desired crystalline structure to the particles, although it also leads to some agglomeration [28]. Depending on the heat treatment procedure, the final product may end up in the form of a nanometer-scale powder or bulk material. The size, shape, and structure of the final product are greatly influenced by the reaction parameters.

Thus, the sol–gel process has seven steps: (1) preparing of required solution, (2) formation of a stable metal precursor solution (sol), (3) formation of a gel by a polycondensation reaction (gel), (4) aging the gel for hours to days resulting in the expulsion of solvent, Ostwald ripening and formation of a solid mass, (5) drying the gel of any liquids, (6) dehydration and surface stabilization, and (7) heat treatment of the gels to generate crystalline nanoparticles. Details of the sol–gel process are discussed more extensively in several excellent review articles [18, 28, 57, 99].

Up to now, most publications related to the sol–gel synthesis have been confined to the preparation of ultrafine metal oxide powders or thin films. Reports on the sol–gel synthesis of nanosized sulfides, selenides, or tellurides are relatively much

scarcer. However, despite this, when using sol–gel processing, a lot of different II-VI compounds such as CdS [47, 140, 160, 186], CdTe [116], CdSe [5, 49], ZnS [19, 188], ZnTe [172], various nanocomposites [58], and doped II-VI semiconductors [116, 172] were synthesized. It is important to note that studies by Starnic et al. [188] during the sol–gel synthesis of ZnS showed that the gel formed during this process is indeed a ZnS gel. The following reaction mechanism can be proposed for the formation of ZnS gel:

$$\mathrm{Zn-OR + H_2S \rightarrow \quad -\,-Zn-SH + ROH} \tag{11.5}$$

$$\mathrm{Zn-SH + RO-Zn-\,-\rightarrow \quad -\,-Zn-S-Zn-\,+ROH} \tag{11.6}$$

$$\mathrm{Zn-SH + HS-\,-Zn-\,-\rightarrow \quad -\,-Zn-S-Zn-\,-\,+ H_2S\uparrow} \tag{11.7}$$

Currently, there are two sol–gel routes that are used most commonly in the preparation of metal chalcogenides. The first one involves a modified sol–gel route in which the conventional alcohol sol is exposed to a stream of $H_2S$ or some other source of chalcogens. The other one is the use of thiols instead of alcohol for the formation of sulfides or selenides by a modification of the first sol–gel route. It should be noted that, in addition to inorganic precursors, metal-organic precursors may also be used in the sol–gel process. Taurino et al. [195] believe that the choice between these two classes should be based on a number of factors. First, metallorganic precursors are more expensive, and the sol preparation requires sometimes the use of organic solvents [143], such as 2-methoxyethanol, that require careful handling and disposal due to their combined toxicity and high vapor pressure [28]. At the same time, handling of inorganic precursors does not generally require any special equipment such as a glovebox. Their chemistry is also more extensively known and more easily manipulated than that of metal-organic precursors, and the spin coating of their solutions does not require any special conditions such as low moisture. Additionally, the solutions have long-term stability against the increase of viscosity. On the other hand, films prepared from solutions based on metal-organic precursors are much more uniform than those when using inorganic precursors, and they can be easily deposited onto various substrates, including silicon. The organometallic precursors also do not contain possible contaminants such as chlorine or sulfur.

As an example, we describe several processes of sol–gel synthesis of CdS NPs. In a process developed by Munirah et al. [140], cadmium acetate $(CH_3COO)_2Cd{\cdot}2H_2O$ and thiourea $(NH_2CSNH_2)$ dissolved in 2-methoxyethanol separately and kept for constant stirrer for 2 h were used as Cd and S sources, respectively. After then, these solutions were mixed together. The cadmium acetate and thiourea concentration was 1.0 M. Monoethanolamine (MEA: $H_2N(CH_2)_2OH$) was added to obtain the desired sols. To gain the thermal stability, solution was aged for 3 h. Fresh solution was applied to the substrate. Finally, the samples were annealed at a temperature of 200 °C for 2 h. The grain size of CdS NPs from SEM estimations was ~10–12 nm.

Rathinama et al. [160] prepared CdS sol–gel using the following two solutions. Solution I was prepared by mixing 0.6 ml polyethylene glycol, 0.5 ml acetic acid, and 8.9 ml ethanol and stirred for 1 h. Solution II was prepared by mixing 0.1 M cadmium nitrate and 0.2 M thiourea in 100 ml ethanol, and it was also stirred for 1 h. Solutions I and II were mixed and stirred again for 4 h to obtain the final sol – gel used for preparing the film. Continuous film was formed onto the substrates by spin deposition of CdS sol–gel. The films were subjected to subsequent annealing in air at 473 K, 573 K, and 673 K. The measurements showed that synthesized CdS nanocrystallites had hexagonal crystal phase and the size increased from 7 to 14 nm with an increase in the annealing temperature from 473 to 673°C.

It was found that, as for other wet chemical methods of II-VI compound synthesis, the result of the sol–gel process strongly depends on the composition of the solution and the presence in it of such components as capping agents or stabilizers, catalyst, and mineralizers. For example, by synthesizing CdS without surface coating agents, Guglielmi et al. [59] obtained CdS nanoparticles that crystallize into a zinc blende cubic structure with an average crystal size of about 3 nm. Instead, CdS particles prepared using (3-mercaptopropyl)trimethoxysilane (MPTMS) had a hexagonal wurtzite-type structure and were significantly smaller in size.

Arachchige and Brock [5] used standard room temperature inverse micellar strategies to prepare CdSe nanoparticles. These nanoparticles were complexed with the thiolate ligands, 4-fluorobenzenethiol (inverse micellar route), and dispersed in acetone or methanol, respectively, to make orange-red colored CdSe sols. They established that if the natural process of photooxidation is used, then gel formation occurs within 4–5 weeks. On the other hand, the use of chemical oxidant (tetranitromethane or $H_2O_2$) leads to gelation within 1–2 h.

However, it should be recognized that the sol–gel process is not the dominant method for the synthesis of II-VI semiconductor nanoparticles. It turned out that the sol–gel technology is more efficient in the synthesis of $SiO_2$ or metal oxide matrices incorporated with nanoparticles of II-VI compounds. Currently, there are reports of synthesis $SiO_2$:$Hg_xCd_{1-x}S$ [58], $SiO_2$:CdSe [120], ($SiO_2$-$P_2O_5$):CdSe [45], $SiO_2$:CdS [48, 86], $SiO_2$:CdTe [112, 145], $SiO_2$:ZnSe [63, 77], $SiO_2$:ZnS [13], $ZrO_2$:CdTe [222], and (95$SiO_2$–5$B_2O_3$):ZnSe [118] структур. The sol–gel matrices doped with semiconductor nanoparticles can be made by synthesis of the semiconductor particles directly in a sol containing functionalized alkoxides [86, 145]. For example, Nogami et al. [145] synthesized CdTe NCs-doped silica glasses using the following stages: $Si(OC_2H_5)_4$ was hydrolyzed by adding it dropwise to a mixed solution of $H_2O$, HCl, and $C_2H_sOH$ in the molar ratio 1:0.0027: 1 per mole of $Si(OC_2H_5)_4$. After the solution was stirred for 1 h, $Cd(CH_3COO)_2{\cdot}2H_2O$ and Te or $CdTeO_4$ (dissolved in concentrated $HNO_3$) were added, followed by 1 h of stirring at room temperature. The resultant homogeneous solution was hydrolyzed by adding a mixed solution of $H_2O$ and $C_2H_5OH$. In this second hydrolysis reaction, a molar ratio of 4:1 per mole of $Si(OC_2H_5)_4$ was maintained. After the solution had been stirred for 1 h, it was poured into a polystyrene container and left for about 1 week until it formed a stiff gel. The gel was then further dried (uncovered) for 1 week at room temperature. This

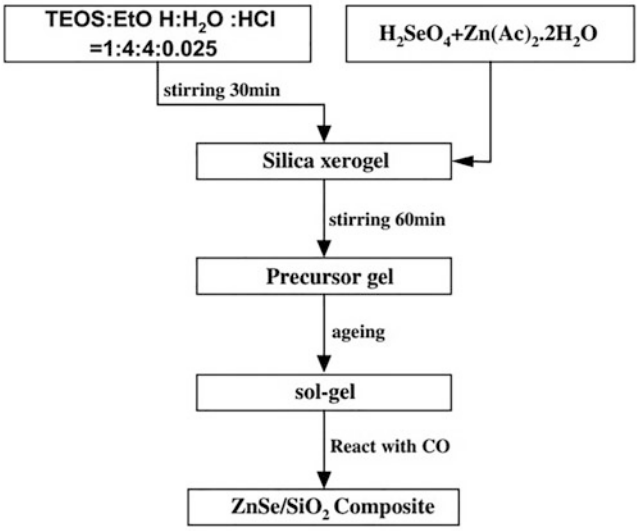


**Fig. 11.6** Flow chart of preparation of $ZnSe/SiO_2$ nanocomposites. (Reprinted with permission from Ref. [63]. Copyright 2007: Elsevier)

dried gel was heated at 150°C in the atmosphere of $H_2$-$N_2$. The crystalline morphology of CdTe NPs in $SiO_2$ matrix was nearly spherical, and average diameters were determined as 5.0 and 8.0 nm for samples heated for 5 h at 400 and 500 °C in $H_2$-$N_2$ gas, respectively. Hao et al. [63] also used direct synthesis of ZnSe nanoparticles in a sol of alkoxides. This sol–gel process is shown in Fig. 11.6. The final treatment to promote the formation of the ZnSe/silica nanocomposite was annealing at a temperature of 500 °C (3 h) in a CO-reducing gas atmosphere. ZnSe nanocrystals were spherical with the average radius of about 4–10 nm. The size of doped ZnSe nanocrystals depended on the annealing time, annealing temperature, and the molar ratio of $ZnSeO_4$ in sol–gel glass.

However, the experiment showed that the synthesis of the nanoparticles separately from the sol–gel medium is more optimal [48]. This makes it possible to use various techniques developed in colloid chemistry to more effectively control parameters that directly affect the properties of final composite materials, such as chemical composition, average size and particle size distribution, electronic state of the surface, and the concentration of the particles in the matrix. That is why in most cases a two-step process is used. For example, Guglielmi et al. [58] first synthesized sulfide sol through a simple chemical method and silica sol via sol–gel process, which were then mixed in the right proportion, and after the completion of the process, the gel synthesized and dried at $T = 60$ °C was annealed at a temperature up to 300 °C. Gacoin et al. [48] used a similar strategy. The incorporation of the CdS particles in the sol was directly achieved by adding the CdS colloidal solution to the

silica sol. Colloidal CdS nanoparticles were synthesized by precipitation method. In order to prevent the irreversible flocculation of CdS colloidal particles in the silica sol, they used a functionalized alkoxide F-$RSi(OEt)_3$. This alkoxide allows the stabilization of the CdS particles through their grafting to the silica network. Lifshitz et al. [120] used a slightly different sequence for the synthesis of $SiO_2$:CdSe structures. They first synthesized selenium-doped silica sol via the sol–gel process and Cd-containing sol, which were deposited in layers on the surface of the substrate and, after drying, were annealed at 400 °C (1.5–2 h). During the indicated thermal treatments, the $SeO_2$ sublimed through the upper layer and reacted with the cadmium acetate to form CdSe. CdSe nanoparticles with a size of 4–6 nm, embedded in a silica sol–gel matrix, had high crystallinity with bulk cubic crystallographic structure. Feraru et al. [45] proposed a very simple way to make a ($SiO_2$-$P_2O_5$):CdSe. To incorporate CdSe into a silicophosphate film, they suggested using pre-synthesized CdSe NPs, which were directly added to the silicophosphate solution. The CdSe-doped silicophosphate solution was kept at room temperature. The gelification occurred on the ninth day. The gel was dried at room temperature in air and then thermally treated at temperatures from 200 to 550 °C for 2 h. Li and Qu [112] used the same approach in the synthesis of $SiO_2$:CdTe composite. However, instead of CdTe powders, they used CdTe QDs.

Sol–gel method has various advantages. First, the mixing of starting reagents at the atomic/molecular level leads to faster reaction times at lower temperatures, which helps to reduce the interdiffusion from one phase into another and the formation of parasitic phases. Since the process starts with a relatively homogeneous mixture, the final product is a uniform ultrafine porous powder. In addition, it allows you to adjust the particle size by simply changing the gelation time. Sol–gel processing also has the advantage that it can be expanded for industrial-scale production. In addition, the sol–gel process also allows the coating of substrates with complex shapes on the nanometer to micrometer scale, which cannot be achieved with some commonly used coating processes. Moreover, sol–gel is suitable the manufacture of thick porous ceramics required for various sensor applications, since the reaction proceeds with the coexisting solvent phase in which evaporation leaves numerous cavities.

On the other hand, sol–gel process can have some disadvantages. These disadvantages include the following:

The cost of the raw materials (the chemicals) can be high:

- Long process duration
- Shrinkage of a wet gel upon drying, which often leads to fracture due to the generation of large capillary stresses and, consequently, makes difficult the attainment of large monolithic pieces
- Difficulties in the process chemistry with respect to properties control and reproducibility
- Difficult to avoid residual OH groups

## 11.5 Hydrothermal Technique

Hydrothermal synthesis is a potentially superior method for low-cost production of II-VI semiconductors, including advanced multicomponent materials and nanocomposites for various applications, since powders of complex II-VI semiconductor can be synthesized directly. Its main feature is the use of water as the solvent [109]. Since water is an exceptional solvent, it is possible to dissolve even nonionic compounds at high-pressure and high-temperature conditions involved in the hydrothermal process. In high-temperature and high-pressure hydrothermal systems, the properties of water will produce the following changes [213]: (1) the ionic product increases, and the ionic product of water rapidly increases with the increase in pressure and temperature. Under high-temperature and high-pressure hydrothermal conditions, the hydrolysis reaction and ion reaction rates will naturally increase with water as the medium. (2) The viscosity and surface tension of water decrease as the temperature increases. In hydrothermal systems, the viscosity of water decreases, and the mobility of molecules and ions in solution greatly increases, such that crystals grow under hydrothermal conditions faster than under other conditions. (3) The dielectric constant of the water solution is often low, and the dielectric constant generally decreases with increasing temperature and increases with increasing pressure. Under hydrothermal conditions, the reaction is mainly affected by temperature, and the dielectric constant of water is significantly reduced. (4) The density decreases, and properties, such as the viscosity, dielectric constant, and solubility of the material, increase with increasing density while the diffusion coefficient decreases with increasing density. (5) The vapor pressure increases and accelerates the reaction by increasing the chance of collision among molecules.

To create such conditions, the precursor with water is placed in an autoclave (see Fig. 11.7). Thus, this chemical process in solution can be easily distinguished from other processes such as sol–gel and co-precipitation by temperature and especially pressure [21]. The temperatures during hydrothermal synthesis are in the range between the boiling point of water (100 °C) and its critical temperature (374 °C), whereas pressures can increase up to 15 MPa. The chemical reaction takes place within a few hours (typically 6–48), leading to the nucleation and growth of nanoparticles. Currently, the production of various particles of II-VI compounds such as CdS [2, 125], CdSe [123, 124], CdTe [20, 228], ZnS [72], ZnSe [144], and ZnTe [228], using hydrothermal process, has been demonstrated. Narrowed band gap II-VI compounds, such as HgTe [164], have also been synthesized hydrothermally.

As an example, we will describe the technological process for the synthesis of CdS microspheres used by Al Balushi et al. [2]. In a typical synthesis process, cadmium acetate dehydrate, ($Cd(CH_3COO)_2 \cdot 2H_2O$), and thiourea, ($SC(NH_2)_2$) were dissolved in deionized water (75 ml) and stirred continuously for 30 min to form a homogeneous solution. Thereafter, the resulting solution was transferred into a Teflon vessel and heated at 160 °C for 12 h in an oven. After the heating process, the Teflon vessel was cooled down up to room temperature, and the deep-yellow

**Fig. 11.7** Tefon-lined stainless steel autoclave used for solvothermal and hydrothermal methods of synthesis. Here, the metal precursors and solvents are premixed and introduced. The steel container is then asserted to a minimum range temperature and pressure. The solutions after treating with temperature and pressure are filtered, washed, and dried to get powdered composites. (Reprinted with permission from Ref. [211]. Copyright 2021: Springer)

powder was collected after centrifugation for 5 min at 5000 rpm. The resulting powder was repeatedly washed with deionized (DI) water and absolute ethanol. Finally, the CdS powder was dried at 80 °C in an oven for 12 h. The average size of CdS crystallites was 26–32 nm. As a rule, the rate of crystal growth is faster at higher temperature. Longer reaction time leads to a larger crystal size. In contrast, higher reactant concentration promotes nucleation and produces smaller crystals [117, 228].

As in other wet chemical methods, the parameters of the synthesized II-VI semiconductors are significantly affected by the composition of the solution and, in particular, the presence of capping agents or stabilizers and mineralizers in it. An appropriate capping agent or stabilizer can be added to the reaction contents at an appropriate time to inhibit particle growth and thus ensure that they are stabilized against agglomeration. The steric or electrostatic stabilization of the reactive molecules affects the nucleation and growth steps, which in turn control the particle size, shape, composition, and crystal structure of the particles. Stabilizers also help dissolve particles in various solvents. As capping agents in the synthesis of II-VI compounds, a long-chain amine, thiol, and trioctylphospine oxide [TOPO], and tri-n-octylphosphine (TOP) can be used. In particular, Schneider and Balan [169] systematized the influence of various capping agents such as ethylene diamine, pyridine, triethanolamine (TEA), cetyltrimethylammonium bromide (CTAB), triethylenetetramine (TETA), trisodium citrate ligand, thiol, and carboxylic acid on the properties of CdSe NPs. They showed that capping agent can determine the structure of synthesized NPs. For example, it was found that hydrothermal synthesis (100 °C, for 10 h) of CdSe QDs from $CdCl_2$ and sodium selenosulfate, $Na_2SeSO_3$, in the presence of ethylene diamine produce a cubic zinc blende CdSe nanoparticles with an average diameter of 12 nm. High-quality CdSe nanorods and fractals can be prepared from $Na_2SeO_3$ and $Cd(NO_3)_2$ at temperatures varying from 100 to 180 °C

when using hydrazine $N_2H_4$ as reductant. Close results were obtained using cetyltrimethylammonium bromide (CTAB) as surfactant during hydrothermal synthesis at 180 °C for 10 h. Dendritic structures and nanoparticles are produced in the absence or at low CTAB concentration, while high CTAB concentration favored the production of nanorods with wurtzite structure (diameter of 40–60 nm and lengths between 200 and 500 nm). Four different morphologies (taper microrods, nanotetrapods, fringy nanostructures, and fasciculate nanostructures) were recently prepared from $Cd(NO_3)_2$, $Na_2SeO_3$, and ethylene diamine tetraacetic acid tetrasodium salt (EDTA) as both a chelating agent and a reductant. Amino acids and small peptides containing a thiol group like cysteine (Cys) and its derivatives and glutathione GSH can also be used to stabilize CdSe QDs in aqueous solution [124]. One can also judge from SEM images for HgTe NPs synthesized under different conditions how strong the influence of solution composition on the structure of the material can be. HgTe nanostructures were synthesized via hydrothermal route by employing Hg(salen) ($H_2$salen = *N,N′*-bis-salicylidene-1,2-ethylenediamine) as a mercury source, $TeCl_4$ and $N_2H_4H_2O$ as the starting reactants at 180 °C for 12 h [164]. Ethylenediaminetetraacetic acid (EDTA) and polyvinylpyrrolidone (PVP) were used as capping agents. $N_2H_4{\cdot}H_2O$ was used as a reductant.

The addition of mineralizers also helps to reduce the size of crystallites [213]. Typical mineralizers are hydroxides (NaOH, KOH, LiOH), carbonates ($Na_2CO_3$), and halides (NaF, KF, NaCl, KCl, LiCl). Different mineralizers result in crystals of different sizes and shapes. For example, Liu and Xue [123] demonstrated that the important factors that influence the morphology of CdSe crystals are the concentration of NaOH, the reaction temperature, and to lesser extent, the concentration of $SeO_3^{2-}$. At low NaOH concentration, the formation of $Se^{2-}$ is slow, which favors the anisotropic nucleation and growth of the CdSe structure along the c-axis (formation of rods). With an increased quantity of NaOH, the concentration of $Se^{2-}$ becomes higher, providing more CdSe building units that grow on nanorods. Sangsefidi et al. [164] also pointed to a strong influence of mineralizers. They found that with variation base from NaOH (Fig. 11.8a) to $NH_3$ (Fig. 11.8d) with keeping the other experimental conditions constant, the morphology of HgTe nanostructure exchanged from rod-shape to agglomeration nanoparticles.

Thus, hydrothermal synthesis is an inexpensive, controllable, reproducible deposition strategy with better nucleation control, so it is considered as an attractive technique to prepare the nanostructures (Aliofkhazraei, 2016). By simply changing the temperature, time, and pressure of the reaction, you can control the particle size, composition, stoichiometry, and particle shape [66, 136]. Moreover, since the properties of the solvent mixture as well as those of the reactants differ intrinsically under high-temperature and high-pressure conditions from their corresponding properties under ambient conditions, the overall result is that this type of processing allows more manipulation of a large set of experimental variables in the synthesis of high-quality nanomaterials [130, 136].

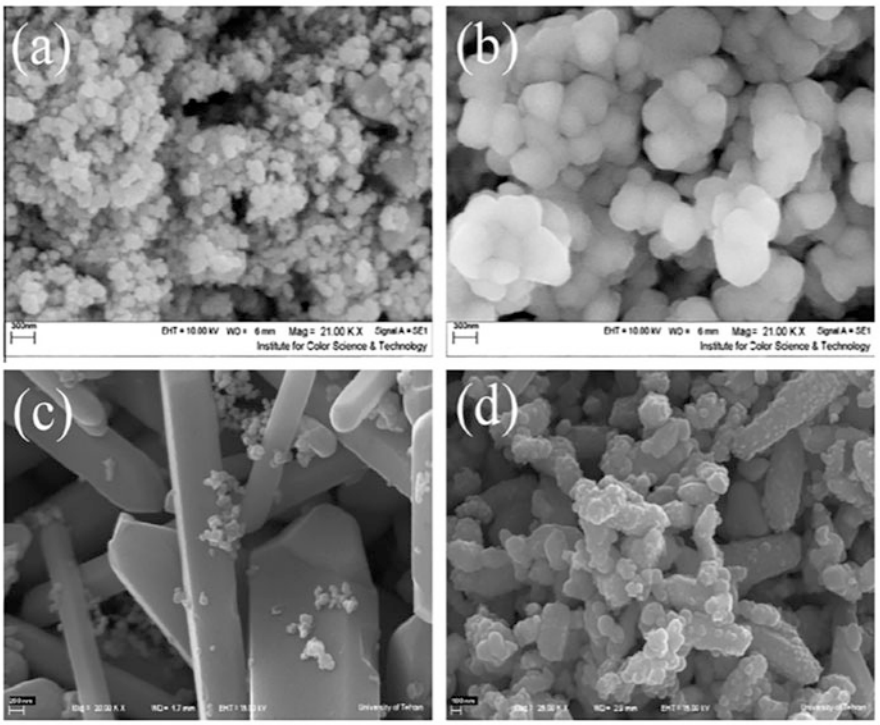


**Fig. 11.8** SEM images of HgTe in presence of (**a**) EDTA and (**b**) PVP as capping agent, $N_2H_4$ as reductant, NaOH as Alkaline agent, (**c**) EDTA as capping agent, Zn as reductant, NaOH as alkaline source, and (**d**) EDTA as capping agent, $N_2H_4$ as reductant, $NH_3$ as alkaline source. (Reprinted with permission from Ref. [164]. Copyright 2013: Elsevier)

One should also note that the calcination step required by earlier discussed techniques can be eliminated in the case of hydrothermal synthesis [21]. However, many of the other steps employed in the previous wet methods can be used in hydrothermal synthesis. Therefore, hydrothermal synthesis with the exception of heat treatment contains the same steps as the sol–gel process. Hydrothermal synthesis generally produces nanoparticles with crystalline structure that are relatively uncontaminated and thus do not require purification or post-treatment annealing but may have a wider size distribution if special treatment for size control is not applied. Other advantages are the use of inexpensive raw materials such as chlorides, nitrates, and organometallic complex. Elimination of impurities, associated with milling and achievement of very fine crystalline powders, is also an advantage of this method.

However, there are also some difficulties connected with hydrothermal synthesis, such as (i) requirement of costly autoclaves, (ii) necessity for high-quality seeds, (iii) high temperature, and (iv) unfeasibility to observe the process during growth. The long duration of the process is also a disadvantage of this method. Insufficient

knowledge for a detailed understanding of the chemistry of complex solutions also creates certain difficulties in the development of hydrothermal synthesis of new materials [136]. To eliminate some of the shortcomings of hydrothermal technique, it was suggested to use this technique in combination with microwave [132, 213] and sol–gel [114]. It was found that indicated approaches allow not only varying the physiochemical and structural properties of the materials but, in addition to that, may lead to the formation of the single-phased materials with improved properties [114].

## 11.6 Solvothermal Technique

The solvothermal process, in which interest has increased significantly in recent years, is an analogue of the hydrothermal process. The main difference between this process and hydrothermal synthesis is the use of organic solvents instead of water as the reaction medium. There are several reasons to stimulate research in this area [216]:

- Firstly, there is a need for technological processes capable to form solid phases with desired properties at intermediate temperatures (100–600 °C). In this regard, the solvothermal method is an appropriate method, as it is a low-temperature process that eliminates diffusion control by using a suitable solvent and limits the reaction to one or more functional groups and leaves most of the chemical bonds intact [176].
- Secondly, the traditional hydrothermal method is limited by the conditions under which some reagents will decompose in the presence of water, or precursors are very sensitive to water, or some reactions will not proceed in the presence of water, which will lead to a failure in the synthesis of the desired compounds. Therefore, it is difficult to obtain many kinds of powders such as carbonides, nitrides, phosphides, silicides, chalcogenides, etc. by a conventional hydrothermal process. The solvothermal process, in which water is replaced by nonaqueous solvents (both polar and polar) such as alcohols, $C_3H_6$, polyamines, $NH_2NH_2$, and liquid $NH_3$, solves this problem and allows the synthesis of compounds that cannot be obtained using hydrothermal synthesis [216]. This means that the so-called solvothermal process can be widely used to obtain various kinds of non-oxide nanocrystalline materials the precursors of which are very sensitive to water. In addition, solvents with a high boiling point are used in solvothermal synthesis, which makes it possible to carry out the growth process without involving high pressures.

As mentioned earlier, in the solvothermal process, one or more types of precursors are dissolved in nonaqueous solvents. The reagents are dispersed in the solution and become more active. The reactions proceed in the liquid phase or in the supercritical state [216]. The solvothermal process is relatively simple and easily controlled by several variable parameters such as solvents, temperature, and reaction

**Table 11.2** Summary of Cd-based chalcogenides synthesized by the solvothermal process

| Compound | Reactants (M/E ratio) | Solvent | Reaction conditions | Symmetry | Shape |
|---|---|---|---|---|---|
| CdS | $CdC_2O_4$+S (2:1) | Ethylenediamine | 120–180 °C, 12 h | Hexagonal | Rod-like |
| | $CdC_2O_4$+S (2:1) | Pyridine | 120–180 °C, 12 h | Hexagonal | Spherical |
| | $CdC_2O_4$+S (2:1) | Ethylene glycol | 160–180 °C, 12 h | Hexagonal | Spherical |
| CdSe | $CdC_2O_4$+Se (2:1) | Ethylenediamine | 140 °C, 12 h | Hexagonal | Rod-like |
| | $CdC_2O_4$+Se (2:1) | Pyridine | 160 °C, 12 h | Hexagonal | Spherical |
| CdTe | $CdC_2O_4$+Te (2:1) | Ethylenediamine | 180 °C, 12 h | Cubic | Rod-like |

*Source:* Data extracted from [216]

time. The sealed system can effectively prevent the contamination of air-sensitive precursors.

Currently, great efforts have been made to synthesize II-VI semiconductors using the solvothermal process [217, 218]. In particular, the group of Yu [216] proposed and investigated several variants of solvothermal reactions for the synthesis of powders of II-VI semiconductors (Eqs. 11.8, 11.9, and 11.10):

$$CdC_2O_4 + E\,(Se, Se, Te) + \text{solvent} \rightarrow CdS(Se, Te) + 2CO_2 \uparrow \tag{11.8}$$

$$Cd^{2+} + NH_2CSNH_2 + \text{solvent} \rightarrow CdS \tag{11.9}$$

$$Na_2S_3 + CdSO_4 + \text{Solvent} \rightarrow CdS + Na_2SO_4 + 2S \tag{11.10}$$

As a solvent they used ethylenediamine (en) and pyridine (py). It was shown that using the proposed solvothermal reactions, it is possible to synthesize nanoparticles of Cd-based compounds with different morphology, particle sizes, and phases. Table 11.2 lists the detained experimental conditions for synthesis of various metal chalcogenides materials by solvothermal reaction between metal oxalates and chalcogens and the characterization of the powders. Examples of other modes of solvothermal synthesis of II-VI compounds are presented in Table 11.3.

It was found that both solvent and temperature play key roles in the reaction, shapes, sizes, and phases (see Fig. 11.9). However, especially solvent has a significant effect on the morphology of the particles. At the same time, it was established that polyamines such as ethylenediamine (en), diethylenetriamine (dien), and triethylenetetramine (trien), which have more than two N-chelating atoms, can be used as "shape-controller" of nanoparticles. For example, it was found that CdS nanocrystallites synthesized by a reaction of $CdC_2O_4$ with S in ethylenediamine at 160–C are uniform nanorods with diameters of 20–50 nm and lengths of 200–1300 nm. In contrast, the particles obtained in pyridine under the same conditions display spherical disc-like shape with a size of 40 nm. It was also found that

**Table 11.3** Examples of solvothermal synthesis of II-VI compound nanoparticles

| II-VI | Precursors | | Solvent | T, °C/t, h | Ref. |
|---|---|---|---|---|---|
| | Metal | Chalcogen | | | |
| ZnS | $Zn(NCS)_2(C_5H_5N)_2$ | | Ethylene glycol | 160–180/12 | [85] |
| | $C_{10}H_{20}N_2S_4Zn$ | | Ethanol | 150–200/12–72 | [226] |
| ZnS: Mn | $ZnCl_2 + MnCl_2$ | S powders | Oleic acid | 180/60 | [225] |
| ZnSe | $ZnSO_4$ | Se elemental | Triethylamine | | [74] |
| | $Zn(Ac)_2$ | $Na_2SeO_3$ | Hydrazine hydrate | 180/1–5 | [242] |
| ZnTe | Zn foils | $TeO_2$ | Hydrazine hydrate | 80/12; annealing 520 °C ($N_2$) | [203] |
| | Zn powders | Te powders | Ethylenediamine + Hydrazine hydrate | 180/6; annealing 290 °C ($N_2$) | [34] |
| CdS | $Cd(NO_3)_2$ | $CH_4N_2S$ | Ethylene glycol | 140/0.1–1 | [113] |
| | $CdSO_4$ | $Na_2S_3$ | Benzene | 80–120 | [218] |
| | $CdCl_2$ | $CH_4N_2S$ | Diethylenetriamine | 220/48 | [33] |
| CdSe | $Cd(NO_3)_2$ | Se [$HNaO_3$] | Ethylenediamine | 180/12–24 | [201] |
| | $Cd(NO_3)_2$ | Se powders | Polyethylene glycol | 200/72 | [155] |
| CdTe | $CdCl_2$ | $K_2TeO_3$ | Ethylene glycol | 150/12 | [230] |
| | $Cd(NO_3)_2$ | Te powders | Ethylenediamine | 200/72 | [189] |

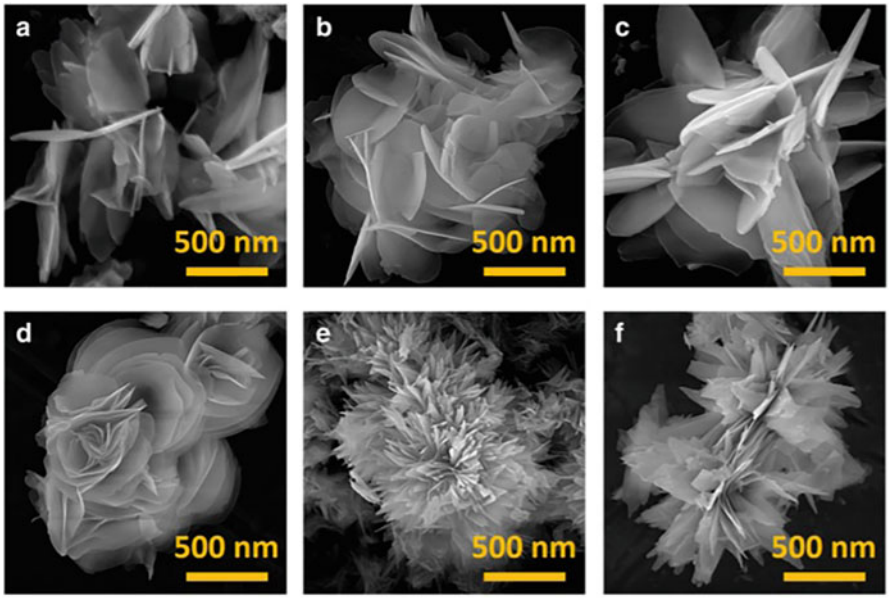


**Fig. 11.9** FESEM images of ZnS nanoflowers prepared by solvothermal synthesis (Zn $(NO_3)_2$ + thiourea + $C_2H_4(NH_2)_2$) + water) during the reaction time of 6 h at the different growth temperatures: (**a**) 100 °C, (**b**) 110 °C, (**c**) 120 °C, (**d**) 130 °C, (**e**) 140 °C, and (**f**) 180 °C. (Reprinted with permission from Ref. [38]. Copyright 2009: Springer)

increasing the temperature and using a solvent with low dielectric constant are beneficial for producing nanocrystalline CdS in hexagonal phase [218]. The water content in the system not only induces the presence of cubic phase CdS nanocrystalline but also leads to a particle size increase. At the same time, Vaquero et al. [200] studied different solvents and found that ethylenediamine is an optimal solvent to control the growth, morphology, and crystal structure of the CdS.

Generally, the size of the particles synthesized during the solvothermal process increases with increasing process temperature. For example, Jiang et al. [85] observed that nanospheres increase in size with increasing reaction temperature, reaching sizes of 200, 350, and 450 nm over a 12 h reaction period at 160 °C, 180 °C, and 200 °C, respectively. Such nanospheres are usually aggregates of many tiny nanocrystals, the size of which can be at the level of 10 nm or less [227]. An increase in the concentration of precursors is also accompanied by the growth of nanoparticles. Wang et al. [206] found that initial precursor concentrations are also key factors in controlling the shape of the resulting CdSe and CdTe nanocrystals, and different shapes such as dot shape, rod shape, and branched shape can be controlled by only changing initial precursor concentrations. The process time also has a significant effect on the parameters of the synthesized nanoparticles. According to Venci et al. [201], an increase in the time of the synthesis of CdSe nanoparticles from 12 to 24 h was accompanied by an increase in the crystallite size from 12 mm to 28 nm. To better control the size and shape of nanocrystals, reducing agent $KBH_4$ [74] and polyvinylpyrrolidone (PVP) as a capping agent [113, 230] can be added to the solution. For example, the addition of PVP helps to reduce the size of nanoparticles [113].

In some cases, annealing in an inert atmosphere is necessary to complete the reaction. Thus, in the synthesis of ZnTe powders, at the final stage after solvothermal synthesis at a low temperature and washing of the synthesized samples, annealing was carried out in a nitrogen atmosphere at a temperature of 290 °C [34] and 520 °C [203].

Thereby, the solvothermal synthesis method is an efficient and facile method for preparing NPs of II-VI compounds. Nanocrystallite of these materials with high crystallinity and good orientation could be obtained by this method. Despite the fact that the method has several advantages, the particle size distribution, purity of nanophase, and morphology variation still remain a challenge to overcome. In addition, as with hydrothermal synthesis, there are some safety issues with this process due to the very high pressure generated in the reactor. Hence, care must be taken when filling the autoclave, which should not exceed 85% by volume (usually 80%). Moreover, the reaction process is unobservable because the reactions take place in a closed reactor and the progress of the reaction is not controlled. Therefore, it is difficult to investigate the mechanism of formation of synthesized nanostructures.

## 11.7 Sonochemical Method

Sonochemistry provides a simple and resourceful method for the chemical preparation of nanomaterials. In sonochemical methods, solution of the starting material (e.g., metallic salts) is subjected to a stream of intensified ultrasonic vibrations (between 20 kHz and 15 MHz), which breaks the chemical bonds of the compounds [190, 221]. The physical phenomenon responsible for the sonochemical process is acoustic cavitation. The ultrasound waves pass through the solution, causing alternate compression and relaxation. This leads to acoustic cavitation, i.e., formation, growth, and implosive collapse of bubbles in the liquid. In addition, the change in pressure creates microscopic bubbles that implode violently, leading to emergence of shock waves within the gas phase of the collapsing bubbles. These bubbles are in the nanometer-size range. Cumulatively, the effect of the collapse of millions of bubbles leads to an excess amount of energy released in solution, which creates the conditions for chemical reactions. Transition temperatures of ~5000 K, pressures of ~1800 atm, and cooling rates above 1010 K/s have been recorded in localized hot spots of cavitation implosion [190]. Studies have shown that ultrasonic irradiation of aqueous liquids leads to the formation of free radicals. The primary products of sonolysis in water are H• and OH• radicals. These radicals can recombine to return to their original form, or combine to produce $H_2$ and $H_2O_2$. They can also produce $HO_2$ in combination with $O_2$. It is these strong oxidizing and reducing agents that are involved in various sonochemical reactions occurring in aqueous solutions.

A typical apparatus that permits easy control over ambient temperature and atmosphere during sonochemical synthesis is shown in Fig. 11.10. Sonochemical decomposition rates for volatile organometallic compounds depend on a variety of experimental parameters such as vapor pressure of precursors, solvent vapor pressure, and ambient gas. In order to achieve high sonochemical yields, the precursors should be highly volatile since the primary sonochemical reaction site is the vapor inside the cavitating bubbles [190]. So that decomposition takes place only during cavitation, thermal stability is also important. In addition, the solvent vapor pressure should be low at the sonication temperature, because significant solvent vapor inside the bubble reduces the bubble collapse efficiency. The excessively high rate of cooling process is found to affect the formation and crystallization of the obtained products [51]. The products could be either amorphous or crystalline depending on the temperature in the ring region of the bubble. Time, energy, and pressure conditions make sonochemistry a distinct process as compared to other conventional methods.

It was shown that the sonochemical synthesis is appropriate and well-organized method for the preparation of metal chalcogenide with controlled nanostructures. In particular, Zhou et al. [234] synthesized CdS nanostructures using sonochemical method with Cd (EDTA) and $Na_2S_2O_3$ in deionized water solution. They found that concentration of ethylenediaminetetraacetic acid (EDTA) greatly affects the process. Concentration of EDTA below 7% produced spherical-shaped CdS NPs, while with 8.5–10.5% concentration, mostly CdS NRs were developed. Semiconductor CdS with nanoporous hollow structure has been prepared utilizing the sonochemical

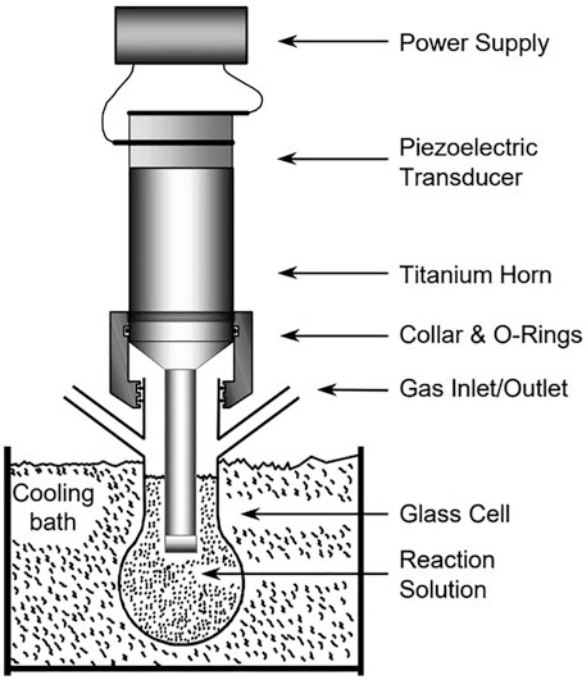


**Fig. 11.10** A typical sonochemical apparatus with direct immersion ultrasonic horn. Ultrasound can be easily introduced into a chemical reaction with good control of temperature and ambient atmosphere. The usual piezoelectric ceramic is PZT, a lead zirconate titanate ceramic. Similar designs for sealed stainless steel cells can operate at pressures above 10 bar. (Reprinted with permission from Ref. [190]. Copyright 1999: Springer)

method with the help of *Escherichia coli* bacteria as template [177]. The structure of CdS showed a change from cubic to hexagonal form. The hexagonal-structured CdS nanoporous hollow microrods showed unique improvements in photoconversion performance.

Importantly, sonochemical synthesis has been successfully used to synthesize a wide range of II-VI semiconductors. Examples of reported II-VI semiconductors synthesized by this method, besides CdS [6, 17, 61, 177, 187, 207, 234], include CdSe [104, 174], CdTe [78, 111, 131, 163], ZnS [27], ZnSe [237, 239], ZnTe [80], and HgS [238].

The advantages associated with sonochemical methods include uniform size distribution of synthesized nanoparticles, a higher surface area, and faster reaction time. However, problems associated with process scaling, inefficient use of energy, and low yield limit the application of this method.

## 11.8 Microemulsion Technique

Microemulsions or micelles (including reverse micelles) represent an approach based on the formation of micro-/nano-reaction vessels for the preparation of nanoparticles, and they have received considerable interest in recent years [22, 37, 129]. This technique uses an inorganic phase in water-in-oil (w/o) microemulsions, which are isotropic liquid media with nanosized water droplets that are dispersed in a

**Table 11.4** Examples of Cd-based nanostructures synthesized by microemulsion technique

| Material | Surfactant | Oil | Microemulsion scheme with w/o system | Ref. |
|---|---|---|---|---|
| CdS/PMMA nanocomposite | AOT | Methyl methacrylate | Two microemulsion scheme | [116] |
| CdS/PANI nanocomposites | NP5 and NP10 | Cyclohexane | | [96] |
| CdS NRs | TX-100 + hexanol | Cyclohexane | | [226] |
| | IGEPAL | | | [202] |
| CdTe@$SiO_2$ nanospheres | Triton X-100 + n-hexanol | Cyclohexane | One microemulsion scheme | [214] |
| CdSe NRs | AOT + n-hexanol | Hydrazine hydrate | | [219] |
| CdSe nanospheres | CTAB + isobutanol | Cyclohexane | Two microemulsion scheme | [32] |

continuous oil phase. In general, microemulsions consist of, at least, a ternary mixture of water, a surfactant, or a mixture of surface-active agents and oil. The classic examples for emulsifiers are sodium dodecyl sulfate (SDC) and aerosol sodium bis(2-ethylhexyl)sulfosuccinate (AOT). Surfactants such as pentadecaoxyethylene nonylphenylether (TNP-35), decaoxyethylene nonylphenyl ether (TNT-10), polyoxyethylene(5)nonylphenolether (NP5), polyoxyethylene(10) nonylphenol ether (NP10), cetyltrimethylammonium bromide (CTAB), polyoxyethylene tert-octylphenyl ether (Triton X-100), octylphenoxy poly (ethyleneoxy)ethanol (IGEPAL), and many others, that are commercially available, can also be used in these processes. The surfactant (emulsifier) molecule stabilizes the water droplets, which have polar heads and nonpolar organic tails. The organic (hydrophobic) portion faces toward the oil phase, and the polar (hydrophilic) group toward water. In diluted water (or oil) solutions, the emulsifier dissolves and exists as a monomer. However, when its concentration exceeds a certain limit, called the critical micell concentration (CMC), the molecules of emulsifier associate spontaneously to form aggregates called micelles. These micro-water droplets then form nanoreactors for the formation of nanoparticles. Some examples of surfactants and oils used in the synthesis of II–VI nanoparticles are listed in Table 11.4.

A typical method for preparing II-VI semiconductor nanoparticles in micelles is to form two microemulsions, one with the metal salt of interest and the other with the chalcogen precursor, and mix them together [129]. Various metal salts can be used as a source of metal ions, such as $CdSO_4$, $Cd[NH_3]_4SO_4$, $ZnCl_2$, $Cd(CH_3COO)_2$, $CdCl_2$, $Cd(NO_3)_2$ $Cd(ClO_4)_2$, etc., and both elemental Zn, Cd, S, Se, and Te, as well as salts containing chalcogen, such as $Na_2SeSO_3$, $Na_2SO_3$, NaHSe, $Na_2S$, $H_2Te$, $(NH_4)_2S$, $Na_2TeO_3$, and $Na_2SeO_3$, etc., can be used as a chalcogen precursor. The microemulsion reaction can easily be carried out at room temperature, and no aggregation occurs between the NPs due to the presence of surfactant material. A

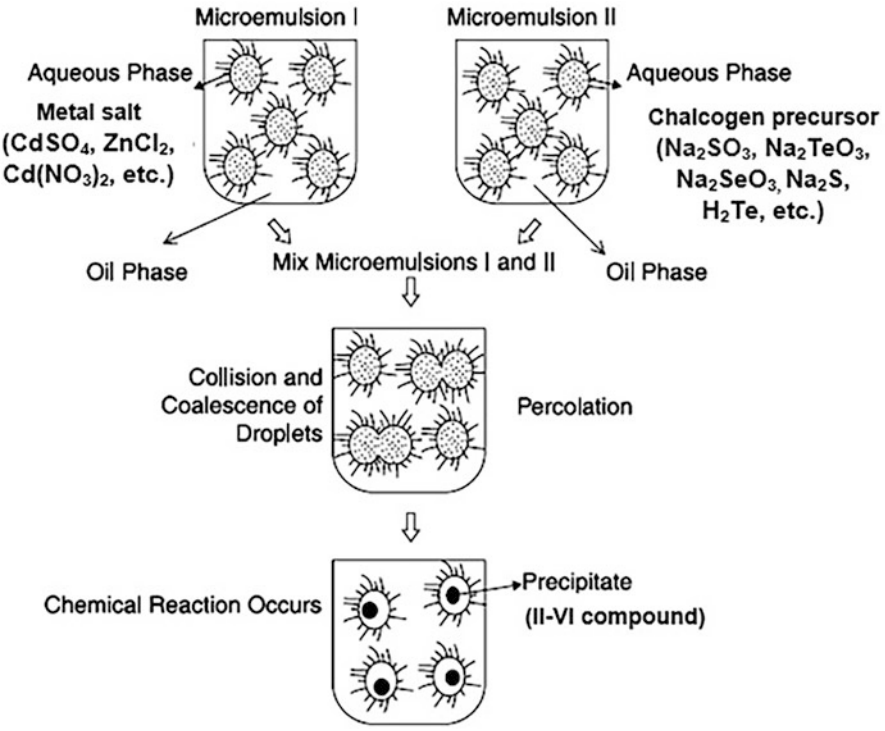


**Fig. 11.11** Proposed mechanism for the formation of metal particles by the microemulsion approach using two microemulsion scheme. (Adapted with permission from Capek [22]. Copyright 2004: Elsevier)

schematic diagram is shown in Fig. 11.11. When two different reactants mix, the interchange of the reactants takes place due to the collision of water microdroplets. Once a nucleus forms with the minimum number of atoms, the growth process starts. Nanoparticle synthesis inside the micelles can be achieved by different methods, including hydrolysis of reactive precursors, such as alkoxides, and precipitation reactions of metal salts [129]. The reaction (reduction, nucleation, and growth) takes place inside the droplet, which controls the final size of the particles. The interchange of the reactant is very fast, so for the most commonly used microemulsions, it occurs just during the mixing process. The reactant concentration has a major influence on the reduction rate. The interchange of nuclei between two microdroplets does not take place due to the special restrictions from the emulsifier. Once the particle inside the droplets attains its full size, the surfactant molecules attach to the metal surface, thus stabilizing and preventing further growth. Solvent removal and subsequent calcination lead to the final product.

The experiment showed that the microemulsion method provides the ability to manipulate the size and shape of nanoparticles by adjusting parameters, such as concentration and type of surfactant, the type of continuous phase, the concentration of precursors, and molar ratio of water to surfactant [129, 184]. This means that this

method allows the preparation of various morphologies and intricate nanostructures. Therefore, the microemulsion technique is very useful for the preparation of the nanomaterials with required properties including the geometry of the particles, the surface area, and most importantly the homogeneity of the obtained material. For example, Holmes et al. [73] demonstrated size control of CdS NPs by varying the ratio of water to surfactant. Zhang et al. [226] have shown the possibility of forming nanorods (NRs) and nanofibers by microemulsion synthesis method. The size of the NRs has been dependent on the concentration of the reagents used and defined the limit of concentration. In general, a higher water content provided a wider dispersion of NRs. It has also been shown that using the microemulsions method nanocomposites can be formed. For example, Li et al. [116] synthesized a CdS/PMMA nanocomposite using this method, and Khiew et al. [96] synthesized PANI/CdS nanocomposite.

The microemulsion method also allows the synthesis of core/shell structures. In particular, Hao et al. [65] synthesized CdSe/CdS nanomaterials, and Song et al. [185] and Aubert et al. [7] synthesized CdTe/CdS and CdTe/CdS/$SiO_2$ core/shell structures. The resulting core/shell QDs (with diameter 64 nm) were found inert and chemically established even in insensitive environments as a consequence of the silica layer. CdTe NCs encapsulated in silica spheres (CdTe@$SiO_2$) as core-shell-structured spheres have been synthesized by hydrolysis and microemulsion by Yang and Gao [214]. There are also reports indicating the synthesis of CdS/ZnS [71], CdS/HgS [87], $Ag_2S$/CdS [62], and CdSe/ZnS structures [154]. The ability to control the formation of different kinds of core-shell structures with sub-nanometric resolution is considered to be the main advantage of this method. A literature survey depicts that the ultrafine nanoparticles in the size range between 2 and 50 nm can be easily prepared by this method [129, 184]. Hollow-structured CdSe NPs have been also prepared via microemulsion technique [32].

Disadvantages include low production yields and the need to use a large amount of solvents and surfactants: this method requires several washing processes and further stabilization treatment due to the aggregation of the obtained nanoparticles [22, 129]. Modifications have been made to overcome these shortcomings. For instance, reverse microemulsion technique has been developed [37]. The synthesis of II-VI compounds from reverse micelles is similar in most aspects to the synthesis of these materials in aqueous phase by the precipitation process.

In order to solve some of the problems of the microemulsion method, the combination of microemulsion with some other synthetic methods has been reported in recent decades. For example, it has been shown that the combination of sonochemistry and microemulsions or micelles can be an effective method for the synthesis of various types of nanostructures. The cavitation behavior of ultrasonic radiation can lead to extraction, mixed-phase reactions, and emulsification in a heterogeneous liquid-liquid system. Thus, under ultrasonic irradiation, it is possible to emulsify liquid-liquid heterogeneous systems with the formation of microemulsions. Using this approach, Huang et al. [75] synthesized spherical assemblies of nanocrystalline CdS particles.

## 11.9 Microwave-Assisted Method

Microwave irradiation is electromagnetic irradiation in the frequency range of 0.3–300 GHz, (wavelengths of 1 mm to 1 m). Therefore, the microwave region of the electromagnetic spectrum lies between infrared and radio frequencies. The microwave method is gaining more and more interest because it requires relatively little energy and time [8, 107, 134]. In this synthesis method, a definite quantity of precursors mixed solution enclosed in a special vessel and heated up in a microwave absorption oven by means of microwave irradiation. As it stated above, in spite of benefits of wet chemical routes for synthesis of II-VI semiconductor NPs, as a rule, they need a long time for synthesis. Microwave processing has attracted a lot of attention due to its advantages of providing faster synthesis rate, resulting superior to traditional heating. Indeed, since microwaves can penetrate the material and supply energy, heat can be generated throughout the volume of the material, resulting in volumetric heating. Microwave-assisted methods involve rapid and uniform heating of the reaction medium with no temperature gradients through two mechanisms: dipolar polarization and ionic conduction. The ability to elevate the temperature of a reaction well above the boiling point of the solvent increases the speed of reactions by a factor of 10–1000. As a result, the reaction times are reduced from a few hours to several minutes or even seconds without compromising the purity or particle size [162]. The effect of microwave irradiation on the synthesis process has not yet been studied. Quick changes due to electric and magnetic forces directions, friction, and collisions of molecules are observed [110]. Thermal effects of microwave irradiations include consistent heating and superheating, while nonthermal effects have not been properly understood. It is considered that microwave irradiation reduces the activation energy of the materials and consequently provides a quick growth mechanism. Faster reaction rates favor rapid nucleation and formation of small, highly monodisperse particles. Yields are also generally higher, and the technique may provide a means of synthesizing compounds that are not available conventionally [168]. Additionally, the method can lead to the synthesis of materials with smaller particle size, narrow particle size distribution, high purity, and enhanced physicochemical properties [138]. Furthermore, microwave methods are unique in providing scaled-up processes without suffering thermal gradient effects, thus leading to a potentially industrially important advancement in the large-scale synthesis of nanomaterials [151]. Therefore, it is not surprising that microwave processes have been used to synthesize different highly crystalline nanoparticles of pure and doped II-VI compounds. Examples of microwave-assisted synthesis modes of Cd-based II-VI compounds are listed in Table 11.5. Other II-VI semiconductors, such as wide bandgap compounds ZnS [93], ZnSe [183], ZnTe [178], and narrow gap HgS [119, 208], have also been synthesized using a microwave-assisted process.

As in all wet chemical methods of NPs synthesis, the parameters of the synthesized materials are highly dependent on temperature, time, and reagents molar ratio [67, 68]. The value of pH of the solution is also an important parameter to be considered; the optimal value of pH for this method is 8–10 [110].

**Table 11.5** Cd containing II-VI semiconductor nanomaterials prepared through microwave-assisted method using different synthesis conditions

| Material | Power/ frequency | Precursors | Irradiation time | pH | Ref. |
|---|---|---|---|---|---|
| CdS NTs | 10 W/ 2450 MHz | $Na_2S$ and $CdSO_4$ | – | – | [175, 177] |
| CdS NPs | 1300 W/ 2.4 GHz | Thioacetamide ($CH_3CSNH_2$) and $CdCl_2$ | 60 s | 8 | [171] |
| CdS and CdS:Cu NPs | 720 W/ 2.45 GHz | $CdCl_2{\cdot}5H_2O$, $CH_2CSNH_2$ and Cu $(CH_3COO){\cdot}2H_2O$ | 1–15 min | – | [165] |
| CdSe NCs | 900 W/ 2.43 GHz | $CdSO_4$, potassium nitriloacetate, and $Na_2SeSO_3$ | 30–60 min | – | [237, 239] |
| CdTe QDs | 400 W/ 2450 MHz | $CdCl_2$, $Na_2TeO_3$, $NaBH_4$, and 3-mercaptopropionic acid (MPA) | 10–40 min | – | [35] |
| CdSe–CdS QDs | 0–1000 W/ 2450 MHz | $CdCl_2$, NaHSe, and MPA | 5–60 min | 9 | [150] |
| CdTe/CdS CShs | 0–300 W/ 2450 MHz | $CdCl_2$, $Na_2S$, NaHTe, and MPA | – | 8.4 | [69] |
| CdS/CdSe QDs | 0–1000 W/ 2450 MHz | $CdCl_2$, NaHSe, and MPA | 30 min | 9 | [223] |
| ZnS/CdSe | 880 W/ 2.44 GHz | $Cd(stearate)_2$, Se, stearic acid, Zn $(Un)_2$, CySCN, octylamine | 30–120 s 30 s | – | [240] |
| (PVP)-capped CdS NPs | 1000 W/ 2450 MHz | $Cd(Ac)_2$ and thiourea in N, N-dimethylformamide (DMF) | 30 s with cycles | – | [70] |

*Source*: Data extracted from Majid and Bibi [126]

At present, microwave heating seems to be the most promising way to achieve short synthesis times. Microwave energy is precisely controllable and can be turned on and off instantly, eliminating the need for warm-up and cool-down. In addition, automation allows control over the reaction conditions and hence facilitates control of particle size, morphology, and crystallinity [14]. The choice of starting metal oxide precursors (as acetates, chlorides, isopropyls) and solvents (as ethylene glycol, benzene) can govern reaction success, particle size, and crystal structure [15].

Limitations of the microwave-assisted processes are associated with the instrumental apparatus itself. The possibility of varying the reaction conditions by finely tuning/controlling the irradiation power and the temperature are the main drawbacks that, in some cases, may hinder reproducibility, especially when not laboratory-designed microwave ovens are used [134]. Finally, it should be noted that the articles published so far in the literature on semiconductors of the II-VI group synthesized using a microwave process indicate a lack of comprehensive studies. Many researchers have simply synthesized materials using microwave irradiation and have not focused on understanding the effect of microwave irradiation parameters such as irradiation time, microwave power, etc. on their final properties.

## 11.10 Hot-Injection and One-Step Colloidal Method

The hot-injection method pioneered by Murray et al. [141] to obtain CdSe nanocrystals is an efficient method for the synthesis of high-quality nanocrystals with good crystallinity and narrow size distribution. This simple method only requires the rapid introduction of hot, highly reactive precursors into a hot organic solvent to induce a short burst of nucleation and then subsequent growth into nanocrystals of varying morphology and conditions. However, if we want to achieve better control over the growth of nanocrystals, it is desirable to separate the stages of nucleation and growth [153]. As well as hydrothermal and solvothermal methods, this method has good controllability and reproducibility, but unlike them, it is much faster and much safer, since it is carried out under ambient pressure. However, this method also has disadvantages. They are the following:

(i) Usually, in hot-injection synthesis, the solvents are organic compounds, and the capping agents are often chain organic compounds containing phosphine (such as trioctylphosphine and tributylphosphine). However, these organic compounds are often toxic, unstable at high temperature, and expensive. Thus, solvents which are less toxic, more stable at high temperature, and relatively cheaper are desired.
(ii) Capping ligands are always present on the surface of the product, which may interfere with their use.
(iii) Sometimes a low concentration of precursors is needed to obtain monodisperse nanostructures, which means a low yield.
(iv) Purging of protection gas or Schlink line is necessary to prevent oxidation or water absorption, which complicates operation.
(v) The main drawback with it is the requirements of rapid injection and subsequently fast cooling. It is not easy to realize in industrial production. Consequently, hot-injection synthesis is not suitable for large-scale production. In addition, it performs poorly in synthesis reproducibility [149].

Nevertheless, using hot-injection method, the size and morphology of the synthesized nanocrystals can be effectively controlled by adjusting several experimental parameters, such as the type and ratio of starting reagents, temperature and time of reaction, solvent, blocking ligands, etc. Synthesis usually starts at the temperature 250–300 °C. The process takes 1–4 min. As an example, consider the synthesis of CdSe NPs [24]. The solution of cadmium carboxylate, hexadecylamine (HAD), and 2-octadecene (ODE) was degassed for 1 h at room temperature and 1 h at 100 °C under a nitrogen flow. Under a nitrogen atmosphere, the temperature was raised to the injection temperature, and TOPSe solution was injected. The injection temperature was set to 245 °C, and the growth temperature was adjusted at 230 °C. The reaction was stopped by the injection of a solvent at 20 °C. Cadmium carboxylate was prepared by mixing CdO and the stearic or carboxylic acid in a 1:3 molar ratio, degassing for 1 h at 100 °C under a nitrogen flow, and dissolving the cadmium oxide under a nitrogen atmosphere at about 250 °C. The TOPSe solution was prepared by

selenium dissolving in trioctylphospine (TOP). Because of this process, CdSe NPs with the size ~1.5–2.5 nm were synthesized. A more detailed description of this method and its use can be found in the Chaps. 12 and 13 (Vol. 1) and reviews [110].

An important advance over the hot-injection method is the development of a non-injection or one-step colloidal method that does not use the rapid introduction of precursors into solution at high temperature [23, 149, 220, 241]. The precursors are mixed at room temperature and then heated to the reaction temperature. For example, for synthesis of ZnS nanocrystals, 3 mmol of $Zn(acac)_2$ was added into 5 ml of n-dodecanethiol (DDT; $CH_3(CH_2)_{11}SH$) and 25 ml of ODE in a three-necked flask, and then the mixture was heated to 240 °C and kept for 180 min. For synthesis of CdS nanocrystals, 5 mmol of $Cd(acac)_2$ and 30 ml of DDT were added into a three-necked flask, and then the mixture was heated to 200 °C and kept for 23 h [220]. The synthesized ZnS and CdS nanocrystals with cubic zinc blende structure were ~5 nm in size.

Compared to the traditional hot-injection method, processing is simplified while maintaining good control over product properties. Another important notable thing is the selection of precursor. As the precursors are mixed at the first beginning, the reactivity of precursors should be much weaker at room temperature (otherwise the reaction procedure would be out of control), such as the combination of insoluble solid precursors, which are less expensive than high activity precursors. Thus, it is possible to further reduce the cost compared to the hot-injection method.

## 11.11 Photochemical Synthesis

It is known that irradiation with light, especially from the UV region, can change the structure of molecules and cause various photochemical reactions, including photochemical synthesis [41, 182]. A central feature of all light-promoted transformations is the involvement of electronically excited states, generated upon absorption of photons. This produces transient reactive intermediates and significantly alters the reactivity of a chemical compound [92, 182].

In recent years, photochemical synthesis has become widespread in the synthesis of nanostructures of metal chalcogenides of various morphologies [55, 229, 235]. This method has the advantages of mild reaction conditions, and the equipment used is quite simple and cheap, since the well-known low-pressure mercury pillar lamp ($\lambda = 253.7$ nm) and high-pressure indium column-like lamp ($\lambda = 420$–$450$ nm) can be used for these purposes. The processes occurring during the synthesis under the action of UV irradiation in relation to CdSe can be described by the following reactions [236]:

$$SeSO_3^{2-} + e \rightarrow Se^- + SO_3^{2-} \tag{11.11}$$

$$Se^- + e \rightarrow Se^{2-} \tag{11.12}$$

$$Cd^{2+} + Se^{2-} \rightarrow CdSe \tag{11.13}$$

Thus, the formation of CdSe nanoparticles under the action of photoirradiation includes the above three stages: First, $SeSO_3^{2-}$ is reduced to $Se^-$; then $Se^-$ is further reduced to $Se^{2-}$; finally, $Se^{2-}$ reacts with metal cations to form metal selenide nanoparticles. The first reaction may be a slow reaction and the second reaction may be a fast reaction. Using indicated approach Zhu et al. [236] synthesized 7 nm CdSe spherical nanoparticles. For doing this, they irradiated aqueous solution containing $CdCl_2$ and $Na_2SeSO_3$ in the presence of complexing agents for several hours at room temperature. A high-pressure indium lamp was used as the visible photoirradiation source. They have shown that both light intensity and irradiation time have influence on the size of the final products. The complexing agents also play an important role: they can retard the rate of the reactions and cause the particle size to be small. The reactions conducted without complexing agents were unsuccessful.

Studies have shown that this method, in addition to the synthesis of CdSe NPs [212, 229], can be used to synthesize binary CdS [148, 205, 209, 224], CdTe [50, 121], ZnS [54], ZnSe [94, 106], doped QDs [94], ternary compounds [50, 79], and composites [42, 224]. In particular, Wang et al. [209] synthesized CdS nanocrystallites with a cubic or hexagonal phase structure using ultraviolet irradiation. Synthesis proceeded at room temperature by precipitation of $Cd^{2+}$ ions with homogeneously released $S^{2-}$ ions formed during the decomposition of thioacetamide by ultraviolet irradiation. Irradiation time can reach several hours. Usually, the solution is deaerated by continuous $N_2$ bubbling during the whole period of UV irradiation. It has been found that the concentrations of $Cd^{2+}$ and thioacetamide, as well as the solvent, have a great effect on the phase structure, product composition, and average size of CdS nanocrystals. For example, Hao et al. [64] prepared CdS nanocrystals in $C_2H_5OH$ and $H_2O$ solvents using sodium dodecyl sulfate (SDS) as capping agent by ultraviolet irradiation technique. They established that SDS as capping agent in the solvents with different $C_2H_5OH$ and $H_2O$ volume ratios has a great effect on the morphology of the synthesized CdS nanocrystals. At solvent with a $C_2H_5OH/H_2O = 9{:}1$ volume ratio containing 0.2 mol/L, SDS was a favorite medium for the formation of CdS nanorods. While the $C_2H_5OH/H_2O$ volume ratio was changed up to 9.5:1, the dendritic supermolecular CdS nanostructures were obtained. When the $C_2H_5OH/H_2O$ volume ratio was down to 6:1, only CdS nanocrystals with irregular morphologies could be formed. Hao et al. [64] believed that the composition of the solution, i.e., the $C_2H_5OH/H_2O$ volume ratio, influenced such physicochemical properties of the solution as polarity (dielectric constant) and softness, which can affect the dissolution and transport of ions in solution, and thus may lead to the different cap structures of SDS in the formation of CdS nanocrystals. As a result, SDS in different solvents can produce patterns of the different structures. These different patterns can act as suitable nucleation sites or interact with the special crystal planes of the growing CdS nanocrystals, resulting in the formation of CdS nanorods and dendritic CdS nanostructures. Mo et al. [135] observed the same significant effect on the morphologies of CdS NPs (2001). They established a morphology-controlled synthesis of CdS nanocrystallites by introducing poly(vinyl alcohol) (PVA) as the protecting agent, which self-assemble into

desirable shapes. CdS spherical nanoparticles, nanodisks, and nanowires were obtained conveniently, and there were some CdS nanotubes that appeared in the CdS nanodisk sample.

Gao et al. [50] and Zhao et al. [229] have shown that the intensity of UV light, UV irradiation time, pH value of solution, solution temperature, and concentration of anions in solution also play important roles in properties of the photochemically prepared NCs. In Zhao et al. [229], the optimal value of pH for the synthesis of CdSe NPs should be in the range of 10–11. Increasing the irradiation intensity shortens the reaction time, required for the synthesis of nanoparticles of a given size. An increase in the irradiation time and temperature was accompanied by an increase in the size of QDs [94]. Depending on the irradiation time, the size of nanoparticles can vary from 1–2 nm after 10–20 min of irradiation [94] to 25 nm after 48 h of irradiation [212]. In principle, the main conclusions drawn from the study of the photochemical synthesis of CdS and CdSe nanocrystallites can also be applied to other chalcogenides.

## 11.12 Green Synthesis

"Green" synthesis involves the use of a set of green chemistry principles originally defined by Anastas and Warner [3]. Green synthesis developments can be divided into three categories: namely, safety, environment, and efficiency [29]. Safety developments include the development of safer materials and safer processes, i.e., development of less hazardous chemical synthesis using safer chemicals and solvents. Development for the environment includes the development of processes that produce less waste to reduce environmental impact and do not use substances that pose a risk to human health and the environment. As for efficiency, the main thing here is the material and energy efficiency of the processes used, aimed at reducing material and energy costs in the synthesis of the necessary materials. In this regard, the use of aqueous solutions for the synthesis of II-VI compounds, ball milling, and sonochemical and microwave-assisted syntheses can be considered as elements of a "green" technology [95, 157].

However, there is another direction in the synthesis of II-VI compounds, which can literally be attributed to the "green" technology This is the synthesis of II-VI compounds using natural components such as microorganisms (algae, bacteria, fungus, viruses, yeast), and extractions of plants. At present, the combination of nanotechnologies and biotechnologies has formed a promising area for the synthesis of nanomaterials [44, 126]. It has been found that microorganisms and plant extracts are able to use their internal biochemical processes to convert inorganic metal salts into the required NPs [10]. In particular, in 2004, Sweeney et al. found that when $Cd^{2+}$ is added to *E. coli* cultures, *E. coli* binds toxic $Cd^{2+}$ into a Cd-thiolate complex, thereby neutralizing Cd toxicity. Then, if sulfide ions ($Na_2S$) are added, the Cd complex reacts with the added sulfide ions and forms intracellular CdS NPs. The biosynthetic method for obtaining NPs turned out to be harmless compared to all other (physical and chemical) methods. Moreover, it turned out that using this

approach, it is possible to synthesize nanoparticles with small size. For example, using this approach were synthesized CdS NPs with the size ~1 nm [30], 1–2 nm [102], 1.5 nm [233], and 2–5 nm [89, 90].

In a microorganism-based approach, microorganisms such as bacteria [90, 156, 181, 191], fungi [25, 105], and yeasts [4, 26] are cultured in favorable conditions (light, nutrients, pH, temperature, stirring speed). Optimizing all of these culture conditions can significantly increase enzyme activity. Then, a metal salt solution is added to the resulting material and incubated. Synthesis of nanomaterials is observed by visual examination of changes in the color of the culture medium. Microorganisms used in the synthesis of NPs of II-VI compounds are listed in Table 11.6. The mechanisms by which different, natural bacterial strains affect metal chalcogenide NPs precipitation are still largely unclear. However, recent studies on bacterial CdS biosynthesis [199] showed that it is critical to select the correct bacterial strain to precipitate CdS NPs at appreciable yields. Here, synthetic biology provides an exciting means to increase NPs yield and to exert control over the precipitation reaction. For example, in [90], Kang et al. inserted the phytochelatin synthase (SpPCS) gene from the yeast *S. pombe* into *E. coli* to promote $CdCl_2$ precursor intake and thus, increase NP yield.

There are two types of biosynthetic strategies after incubation period: intracellular and extracellular synthesis processes, when the processes occur inside and outside the cell. In extracellular synthesis, centrifugation at various speeds and a washing process are used to get rid of biomass. In an intracellular process, media components and large particles are separated using repeated cycles of sonication, washing, and centrifugation. An extracellular process is preferred over an intracellular one due to the ease of post-processing. It is also more suitable for industrial applications [91]. Finally, after washing with water/solvent (ethanol/methanol), the particles are obtained as bottom granules. A schematic illustration of this method is shown in Fig. 11.12.

With the emergence of a broad range of biosynthetic NP precipitation approaches, there also has been a growing interest in controlling these approaches to affect NP properties. Most strategies to date focus on controlling the particle size, which has large impact on the photoelectronic properties of TM NPs. Already in 1989, when Dameron et al. [30] first precipitated CdS with yeast, they influenced particle size by using different peptide-Cd complexes as precursors, which effectively limited CdS crystallite growth. However, perhaps the simplest way to influence NP size is to control precipitation or incubation time. In particular, Bai et al. [9] found that by changing the culture time, the size of the nanoparticles can be controlled. Cadmium ions were transferred into a living cell from a solution after its incubation at 30 °C in the dark and in an aerobic environment. Testing of the synthesized material showed that the average particle size of CdS was 2.3 nm, 6.8 nm, and 36.8 nm at culture times of 36, 42, and 48 h, respectively. In 2010, Bao et al. [12] showed that the size of extracellularly precipitated CdTe NPs increased predictably with increasing incubation time. Fellowes et al. [43] showed a similar behavior for CdSe NPs when prolonging the refluxing time. There are also studies that show that using biosynthesis can also influence the particle size distribution [89, 90] and NP crystal structure [137].

**Table 11.6** Microorganisms and plant extracts used for biosynthesis of II-VI semiconductor NPs

| Compound | Microorganisn | Name | Location | NPs size, nm |
|---|---|---|---|---|
| CdS | Bacteria | *Escherichia coli*; *A. ferrooxidans*; *A. caldus*; *Stenotrophomonas maltophilia*; *Klebsiella pneumoniae*; *Desulfovibrio alaskensis*; *Thermoanaerobacter*; | Ext. | 2–50 |
| | | *Escherichia coli*; *Pseudomonas*; *Acidithiobacillus thiooxidans* | Int. | 2–20 |
| | Fungi | *Phanerochaete crysosporium*; *Rhizopus stolonifer*; *Pleurotus ostreatus* | Ext. | 2–9 |
| | Algae | *Chlamydomonas reinhardtii*; | Ext. | 2–7 |
| | | *Arthrospira platensis*; *C. reinhardtii*; *C. merolae* | Int | ~8 |
| | Yeast | *Schizosaccharomyces pombe* | Ext., Int. | 2–6 |
| | | Candidas; | Int. | MCs |
| | Enzymes | Cystathionine gamma-lyases; | Cell-free | ~3 |
| | Virus virus | Bacteriophage | Int. | ~40 |
| | Plant extracts | Tomato hairy root extract; *N. tabacum* L. cv.; Fenugreek seed extract; Pomegranate peel extract; Banana peel extract; Hairy root culture of *Linaria maroccana* L; *S. lycopersicum* | n/a | 3–10 |
| CdSe | Bacteria | *Veillonella atypica*; *Bacillus licheniformis* | Int. | 2–4 |
| | Fungi | Helminthosporium solani | Ext. | 3–7 |
| | Enzyme | *Nitrate reductase* | Cell-free | 4–9 |
| CdTe | Bacteria | *Escherichia coli* | Ext., Int. | 2–5 |
| | Fungi | *Rhizopus stolonifer*; *Fusarium oxysporum* | Ext. | 3–20 |
| | Earthworm | *Lumbricus rubellus* | n/a | ~2.5 |
| ZnS | Bacteria | *Klebsiella pneumonia*; *Desulfovibrio desulfuricans*; *R. sphaeroides*; *S. nematodiphila* | Ext. | 18–40 |
| | Fungi | *Fusarium oxysporum*; *Aspergillus flavus*; *S. cerevisiae* | Ext. | 15–60 |
| | Yeast | *Saccharomyces cerevisiae* | Int. | 30–40 |
| | Plant extract | Moringa oleifera leaf extract | n/a | ~30 |

*Source*: Data extracted from [44]
*Int* Intracellular, *Ext.* Extracellular, *MC* mycrocrystals

In the plant-based approach, components, i.e., leaves [84], fruits [39, 233], flowers [133], seeds [196], roots [16, 179], skins (Sasidharan et al., 2014), or other bio entities [152], are extracted through a purification, filtration, and centrifugation. For the synthesis process, a suitable amount of water, a metal salt solution, and various fractions of plant extracts are used. In the process of incubation (3–48 h), simultaneously with a decrease in the concentration of metal salts, the assembly of nanoparticles begins, similar to that observed with the help of microorganisms. In

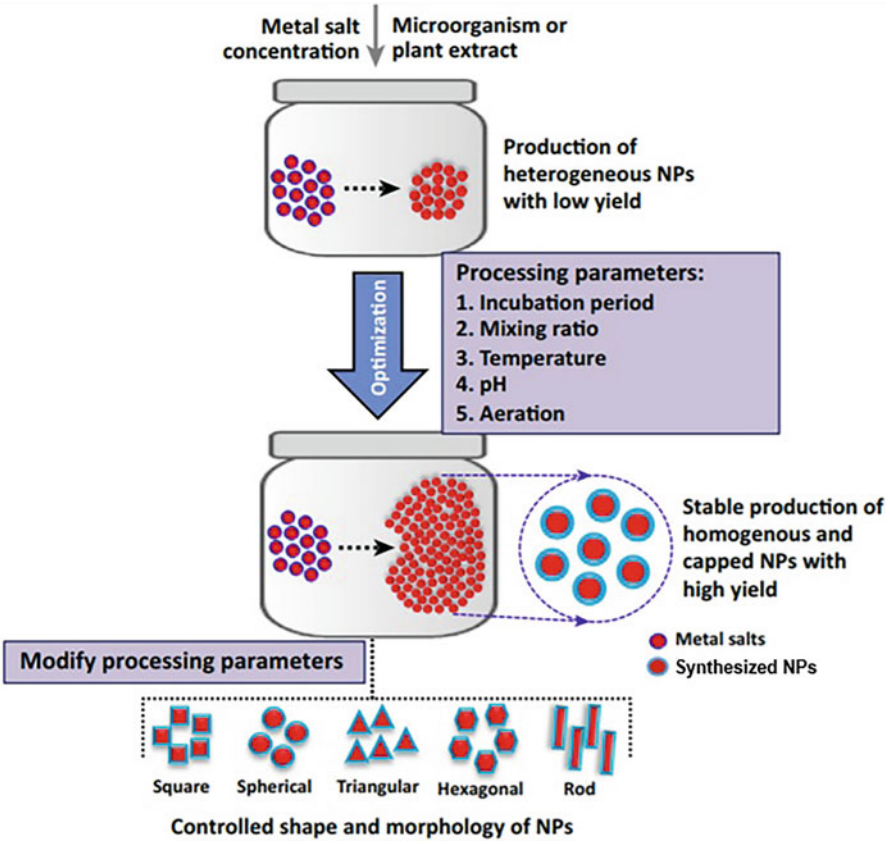


**Fig. 11.12** Parameters of biological synthesis. Synthesis of homogeneous nanoparticles of the same size and shape requires optimization of control parameters, such as salt concentration, mixing ratio of biological extract and metal salt, pH value, temperature, incubation time, and aeration. Biological synthesis can also provide an additional coating layer on the synthesized nanoparticles with the addition of several biologically active groups, which can increase the efficiency of synthesized nanoparticles. (Reprinted with permission from Ref. [180]. Copyright 2016: Elsevier)

plant-based biosynthesis, there are no requirements for well-conditioned culture, expensive isolation methods, or any special, complex, and multistep processes. Several examples of the biosynthesis of compounds II-VI are given in [44, 82, 173, 233]. Zhou et al. [233], synthesizing CdS NPs using banana peel extract as a suitable, harmless, environmentally friendly closure agent, showed that as in all wet chemical processes reaction parameters like quantity of banana peel extract, pH, concentration, and temperature played significant role in NPs formation.

The experiment showed that biosynthesis is really a low-cost technique acceptable for nanoparticle synthesis. It is an environment-friendly technique which provides an extensive variety of environmentally suitable synthesis process. In addition, it is completely free of the poisonous chemical agents and high-energy requirement as in physiochemical methods. As it was shown before, NPs of II-VI compounds can

be synthesized both in bacteria and fungi. However, Jacob et al. [82] believe that fungal-based systems have the advantage of ease of handling and extracellular synthesis. Although bacterial synthesis has an advantage of involving directed evolution or genetic manipulation, fungi have a niche with respect to the cost factor on scale-up and large-scale synthesis. At the same time, Shah et al. [173] believe that in contrast to microorganism, plants approach provides more benefits because it is faster, more cost-effective, and straightforward. This method is more supportive for the synthesis of metal chalcogenide NPs. However, to move to the next stage of development, it is needed to improve the control over size, shape, and complete monodispersivity of the nanostructures. In addition, biosynthetic methods are typically slow and produce particles of low purity, compared with chemical bath deposition methods. While the purity of TM chalcogenide NPs is crucial for some applications, biosynthetic NPs can outperform their pure, chemically synthesized counterparts in other applications. For example, due to the natural presence of organic capping ligands, biosynthetic NPs can bind dye molecules or can bind to other materials, including cells and graphene. This makes them useful as efficient photocatalysts, as natural bioimaging tracers, and as photoabsorbers in energy devices. A more accurate mechanism of biosynthesis is also required for manufacturing of nanomaterials for technological applications. More details on the problems of the synthesis of nanoparticles of II-VI compounds by biosynthetic methods can be found in the reviews [1, 44, 82, 95, 128, 147].

**Acknowledgments** G. Korotcenkov is grateful to the State Program of the Republic of Moldova, project 20.80009.5007.02, for supporting his research.

## References

1. Aguayo OPY, Mouheb L, Revelo KV, Vásquez-Ucho PA, Pawar PP, Rahman A et al (2022) Biogenic sulfur-based chalcogenide nanocrystals: methods of fabrication, mechanistic aspects, and bio-applications. Molecules 27:458
2. Al Balushi BSM, Al MF, Al WB, Kuvarega AT, Al Kindy SMZ, Kim Y, Selvaraj R (2018) Hydrothermal synthesis of CdS sub-microspheres for photocatalytic degradation of pharmaceuticals. Appl Surf Sci 457:559–565
3. Anastas P, Warner J (1998) Green chemistry: theory and practice. Oxford University Press, New York
4. Apte M, Sambre D, Gaikawad S, Joshi S, Bankar A, Kumar AR et al (2013) Psychrotrophic yeast Yarrowia lipolytica NCYC 789 mediates the synthesis of antimicrobial silver NPs via cell-associated melanin. AMB Express 3(1):32
5. Arachchige IU, Brock SL (2006) Sol-gel assembly of CdSe nanoparticles to form porous aerogel networks. J Am Chem Soc 128:7964–7971
6. Arul Dhas N, Gedanken A (1998) A sonochemical approach to the surface synthesis of cadmium sulfide NPs on submicron silica. Appl Phys Lett 72(20):2514–2516
7. Aubert T, Soenen SJ, Wassmuth D, Cirillo M, Van Deun R, Braeckmans K et al (2014) Bright and stable CdSe/CdS@ $SiO_2$ NPs suitable for long-term cell labeling. ACS Appl Mater Interfaces 6(14):11714–11723

8. Baghbanzadeh M, Carbone L, Cozzoli PD, Kappe CO (2011) Microwave assisted synthesis of colloidal inorganic nanocrystals. Angew Chem 50:11312–11359
9. Bai H, Zhang Z, Guo Y, Jia W (2009) Biological synthesis of size-controlled cadmium sulfide NPs using immobilized Rhodobacter sphaeroides. Nanoscale Res Lett 4(7):717
10. Baker S, Harini BP, Rakshith D, Satish S (2013) Marine microbes: invisible nanofactories. J Pharm Res 6(3):383–388
11. Baláž P, Boldižárová E, Godočí E., Briančin J. (2003) Mechanochemical route for sulphide NPs preparation. Mater Lett 57(9):1585–1589
12. Bao H, Lu Z, Cui X, Qiao Y, Guo J, Anderson JM et al (2010) Extracellular microbial synthesis of biocompatible CdTe quantum dots. Acta Biomater 6:3534–3541
13. Bhattacharjee B, Ganguli D, Iakoubovskii K, Sesmans A, Chaughuri S (2002) Synthesis and characterization of sol–gel derived ZnS:$Mn^{2+}$ nanocrystallites embedded in a silica matrix. Bull Mater Sci 25(3):175–180
14. Bilecka I, Niederberger M (2010) Microwave chemistry for inorganic nanomaterials synthesis. Nanoscale 2:1358–1374
15. Bilecka I, Djerdj I, Niederberger M (2008) One-minute synthesis of crystalline binary and ternary metal oxide nanoparticles. Chem Commun 7:886–888
16. Borovaya MN, Naumenko AP, Matvieieva NA, Blume YB, Yemets AI (2014) Biosynthesis of luminescent CdS QDs using plant hairy root culture. Nanoscale Res Lett 9(1):686
17. Bozkurt PA, Derkuş B (2016) Synthesis and characterization of CdS NRs by combined sonochemical-solvothermal method. Mater Sci Poland 34(3):684–690
18. Brinker CJ, Scherer GW (1990) Sol-gel science: the physics and chemistry of sol-gel processing. Academic, San Diego
19. Bu IYY (2013) Sol–gel synthesis of ZnS (O,OH) thin films: Influence of precursor and process temperature on its optoelectronic properties. J Lumin 134, 423–428
20. Bu H-B, Kikunaga H, Shimura K, Takahasi K, Taniguchi T, Kim DG (2013) Hydrothermal synthesis of thiol-capped CdTe nanoparticles and their optical properties. Phys Chem Chem Phys 15:2903
21. Byrappa K, Yoshimura M (2012) Handbook of hydrothermal technology. Elsevier, New York
22. Capek I (2004) Preparation of metal nanoparticles in water-in-oil (w/o) microemulsions. Adv Colloidal Interface Sci 110(1–2):49–74
23. Cao YC, Wang JH (2004) One-pot synthesis of high-quality zinc-blende CdS nanocrystals. J Am Chem Soc 126(44):14336–14337
24. Capek RK, Lambert K, Dorfs D, Frederic P, Smet PF, Poelman D et al (2009) Synthesis of extremely small CdSe and bright blue luminescent CdSe/ZnS nanoparticles by a prefocused hot-injection approach. Chem Mater 21:1743–1749
25. Castro-Longoria E, Vilchis-Nestor AR, Avalos-Borja M (2011) Biosynthesis of silver, gold and bimetallic NPs using the filamentous fungus *Neurospora crassa*. Colloids Surf B: Biointerfaces 83(1):42–48
26. Chen G, Yi B, Zeng G, Niu Q, Yan M, Chen A et al (2014) Facile green extracellular biosynthesis of CdS QDs by white rot fungus *Phanerochaete chrysosporium*. Colloids Surf B: Biointerfaces 117:199–205
27. Cheon SY, Yoon J-S, Oh KH, Jang KY, Seo JH, Park JY et al (2017) Sonochemical synthesis of ZnO-ZnS core-shell nanorods for enhanced photoelectrochemical water oxidation. J Am Ceram Soc 100(9):3825–3834
28. Corriu R, Anh NT (2009) Molecular chemistry of sol-gel derived nanomaterials. Wiley, Chichester
29. Dahl JA, Maddux BLS, Hutchison JE (2007) Toward greener nanosynthesis. Chem Rev 107: 2228–2269
30. Dameron CT, Reese RN, Mehra RK, Kortan AR, Carroll PJ, Steigerwald ML et al (1989) Biosynthesis of cadmium sulphide quantum semiconductor crystallites. Nature 338(6216): 596–597

31. Devi RA, Latha M, Velumani S, Oza G, Reyes-Figueroa P, Rohini M, Yi J (2015) Synthesis and characterization of cadmium sulfide NPs by chemical precipitation method. J Nanosci Nanotechnol 15(11):8434–8439
32. Dong CZ, Zhang LF, Chen S, Zhang MX, Feng L, Cui ZM, Zhang QJ (2013) Hollow structure of CdSe by W/O microemulsion method. In: Advanced materials research, vol 652. Trans Tech Publications, Zürich, pp 215–218
33. Du Y, Zeng F (2013) Solvothermal route to CdS nanocrystals. J Experim Nanosci 8(7–8): 965–970
34. Du J, Xu L, Zou G, Chai L, Qian Y (2006) Solvothermal synthesis of single crystalline ZnTe nanorod bundles in a mixed solvent of ethylenediamine and hydrazine hydrate. J Crystal Growth 291:183–186
35. Duan J, Song L, Zhan J (2009) One-pot synthesis of highly luminescent CdTe QDs by microwave irradiation reduction and their $Hg^{2+}$ −sensitive properties. Nano Res 2(1):61–68
36. Dutková E, Balaz P, Pourghahramani P (2009) CdS NPs mechanochemically synthesized in a high-energy mill. J Optoelectron Adv Mater 11(12):2102–2107
37. Eastoe J, Hollamby MJ, Hudson L (2006) Recent advances in nanoparticle synthesis with reversed micelles. Adv Colloid Interf Sci 128–130:5–15
38. Ebrahimi S, Yarmand B (2019) Morphology engineering and growth mechanism of ZnS nanostructures synthesized by solvothermal process. J Nanopart Res 21:264
39. Edison TJI, Sethuraman MG (2012) Instant green synthesis of silver NPs using Terminalia chebula fruit extract and evaluation of their catalytic activity on reduction of methylene blue. Process Biochem 47(9):1351–1357
40. Elavarthi P, Kumar AA, Murali G, Reddy DA, Gunasekhar KR (2016) Room temperature ferromagnetism and white light emissive CdS: Cr NPs synthesized by chemical co-precipitation method. J Alloys Comp 656:510–517
41. Esser P, Pohlmann B, Scharf H-D (1994) The photochemical synthesis of fine chemicals with sunlight. Angew Chem Int Ed Engl 33:2009–2023
42. Fang Z, Fan Y, Liu Y (2011) Photochemical synthesis and photocatalysis application of ZnS/amorphous carbon nanotubes composites. Front Optoel China 4(1):121–127
43. Fellowes JW, Pattrick RAD, Lloyd JR, Charnock JM, Coker VS, Mosselmans JFW et al (2013) Ex situ formation of metal selenide quantum dots using bacterially derived selenide precursors. Nanotechnology 24:145603
44. Feng Y, Marusak KE, You L, Zauscher S (2018) Biosynthetic transition metal chalcogenide semiconductor nanoparticles: progress in synthesis, property control and applications. Curr Opin Colloid Interface Sci 38:190–203
45. Feraru I, Vasiliu IC, Iordanescu R, Elisa M, Bartha C (2013) Structural characterization of CdSe-doped sol-gel silicophosphate films. Electron Mater Process 49(6):50–56
46. Gao B, Shen C, Yuan S, Yang Y, Chen G (2013) Synthesis of highly emissive CdSe quantum dots by aqueous precipitation method. J Nanomater 2013:138526
47. Gacoin T, Malier L, Boilot J-P (1997) Sol–gel transition in CdS colloids. J Mater Chem 7(6): 859–860
48. Gacoin T, Malier L, Counio G, Boilot J-P (1997) CdS nanoparticles and the sol-gel process. Proc SPIE 3136:358–365
49. Gaeeni MR, Tohidian M, Majles-Ara M (2014) Green synthesis of CdSe colloidal nanocrystals with strong green emission by the sol−gel method. Ind Eng Chem Res 53: 7598–7603
50. Gao X, Wu J, Wei X, He C, Wang X, Guangsheng GG, Qiaosheng PQ (2012) Facile one-step photochemical synthesis of water soluble CdTe(S) nanocrystals with high quantum yields. J Mater Chem 22:6367–6373
51. Gendanken A (2003) Sonpchemistry and its applications in nanochemistry. Curr Sci 85:1720–1722
52. Godočíková E, Baláž P, Gock E, Choi WS, Kim BS (2006) Mechanochemical synthesis of the nanocrystalline semiconductors in an industrial mill. Powder Technol 164(3):147–152

53. Golsefidi MA, Ramandi MF, Shahkooie MAK (2016) Facile synthesis of CdTe nanoparticles and photo-degradation of Rhodamine B and methyl orange. J Mater Sci Mater Electron 27: 12100–12105
54. Gonzalez CM, Wu W-C, Tracy J, Martin B (2015) Photochemical synthesis of size-tailored hexagonal ZnS quantum dots. Chem Commun 51:3087–3090
55. Goto F, Ichimura M, Arai E (1997) A new technique of compound semiconductor deposition from an aqueous solution by photochemical reactions. Jpn J Appl Phys 36(9A):L1146
56. Grundler P (2007) Chemical sensors: an introduction for scientists and engineers. Springer, Berlin
57. Guglielmi M, Kickelbic G, Martucci A (eds) (2014) Sol-gel nanocomposites. Springer, New York
58. Guglielmi M, Martucci A, Fick J, Vitrant G (1998) Preparation and characterization of HgxCd1-xS and PbxCd1-xS quantum dots and doped thin films. J Sol–Gel Sci Technol 11: 229–240
59. Guglielmi M, Martucci A, Menegazzo E, Righini GC, Pelli S, Fick J, Vitrant G (1997) Control of semiconductor particle size in sol-gel thin films. J Sol-Gel Sci Techn 1–3:1017–1021
60. Gupta AK, Kripal R (2012) EPR and photoluminescence properties of $Mn^{2+}$ doped CdS NPs synthesized via co-precipitation method. Spectrochim Acta A 96:626–631
61. Hanifehpour Y, Hamnabard N, Mirtamizdoust B, Joo SW (2016) Sonochemical synthesis, characterization and sonocatalytic performance of terbium-doped CdS NPs. J Inorg Org Polymers Mater 3(26):623–631
62. Han MY, Huang W, Chew CH, Gan LM, Zhang XJ, Ji W (1998) Large nonlinear absorption in coated $Ag_2S$/CdS nanoparticles by inverse microemulsion. J Phys Chem B 102:1884–1887
63. Hao H, Yao X, Wang M (2007) Preparation and optical characteristics of ZnSe nanocrystals doped glass by sol–gel in situ crystallization method. Opt Mater 29:573–577
64. Hao LY, Mo X, Wang CY, Wu Y, Huang DW, Zhu YR et al (2001) Fabrication of CdS nanocrystals with various morphologies in selective solvents via a convenient ultraviolet irradiation technique. Mater Res Bull 36:1005–1009
65. Hao E, Sun H, Zhou Z, Liu J, Yang B, Shen J (1999) Synthesis and optical properties of CdSe and CdSe/CdS NPs. Chem Mater 11(11):3096–3102
66. Hayashi H, Hakuta Y (2010) Hydrothermal synthesis of metal oxide nanoparticles in supercritical water. Materials 3:3794–3817
67. He Z, Zhu H, Zhou P (2012) Microwave-assisted aqueous synthesis of highly luminescent carboxymethyl chitosan-coated CdTe/CdS QDs as fluorescent probe for live cell imaging. J Fluoresc 22(1):193–199
68. He Y, Sai LM, Lu HT, Hu M, Lai WY, Fan QL et al (2007) Microwave-assisted synthesis of water-dispersed CdTe NCs with high luminescent efficiency and narrow size distribution. Chem Mater 19(3):359–365
69. He Y, Lu HT, Sai LM, Lai WY, Fan QL, Wang LH et al (2006) Microwave-assisted growth and characterization of water-dispersed CdTe/CdS core—shell NCs with high photoluminescence. J Phys Chem B 110(27):13370–13374
70. He R, Qian XF, Yin J, Xi HA, Bian LJ, Zhu ZK (2003) Formation of monodispersed PVP-capped ZnS and CdS NCs under microwave irradiation. Colloids Surf A Physicochem Eng Aspects 220(1):151–157
71. Hirai T, Shiojiri S, Komasawa I (1994) Preparation of metal sulfide composite ultrafine particles in reverse micellar systems and their photocatalytic property. J Chem Eng Jpn 27: 590–597
72. Hoa TTQ, Vu LV, Canh TD, Long NN (2009) Preparation of ZnS nanoparticles by hydrothermal method. J Phys Conf Series 187:012081
73. Holmes JD, Bhargava PA, Korgel BA, Johnston KP (1999) Synthesis of cadmium sulfide Q particles in water-in-$CO_2$ microemulsions. Langmuir 15(20):6613–6615
74. Huang S (2006) The study of optical characteristic of ZnSe nanocrystal. Appl Phys B Lasers Opt 84:323–326

75. Huang J, Xie Y, Li B, Liu Y, Lu J, Qian Y (2001) Ultrasound-induced formation of CdS nanostructures in oil-in-water microemulsions. J Colloid Interface Sci 236:382–384
76. Hullavarad NV, Hullavarad SS (2007) Synthesis and characterization of monodispersed CdS NPs in $SiO_2$ fibers by sol–gel method. Photon Nanostr-Fundam Appl 5(4):156–163
77. Hutagalung SD, Loo SC (2007) Zinc selenide (ZnSe) nanoparticles prepared by sol-gel method. In: Proceedings of the 7th IEEE International Conference on Nanotechnology, August, vol 2–5, Hong Kong, pp 930–933
78. Hwang CH, Park JP, Song MY, Lee JH, Shim IW (2011) Syntheses of CdTe QDs and NPs through simple sonochemical method under multibubble sonoluminescence conditions. Bull Korean Chem Soc 32(7):2207–2211
79. Ichimura M, Maeda Y (2015) Conduction type of nonstoichiometric alloy semiconductor CuxZnyS deposited by the photochemical deposition method. Thin Solid Films 594:277–281
80. Ilanchezhiyan P, Mohan KG, Xiao F, Poongothai S, Madhan KA, Siva C et al (2017) Ultrasonic-assisted synthesis of ZnTe nanostructures and their structural, electrochemical and photoelectrical properties. Ultrason Sonochem 39:414–419
81. Iranmanesh P, Saeedni S, Nourzpoor M (2015) Characterization of ZnS nanoparticles synthesized by co-precipitation methodCharacterization of ZnS nanoparticles synthesized by co-precipitation method. Chin Phys B 24(4):046104
82. Jacob JM, Lens PNL, Balakrishnan RM (2016) Microbial synthesis of chalcogenide semiconductor nanoparticles: a review. Microbial Biotechnol 9(1):11–21
83. Jadhav AP, Kim CW, Cha HG, Pawar AU, Jadhav NA, Pal U et al (2009) Effect of different surfactants on the size control and optical properties of $Y_2O_3$:$Eu^{3+}$ nanoparticles prepared by co-precipitation methods. J Phys Chem C 113(31):13600–13604
84. Jemal K, Sandeep BV, Pola S (2017) Synthesis, characterization, and evaluation of the antibacterial activity of allophylus serratus leaf and leaf derived callus extracts mediated silver NPs. J Nanomater 2017:4213275
85. Jiang L, Yang M, Zhu S, Pang G, Feng S (2008) Phase evolution and morphology control of ZnS in a solvothermal system with a single precursor. J Phys Chem C 112:15281
86. Julián B, Planelles J, Cordoncillo E, Escribano P, Sanchez C, Aschehoug P et al (2007) Gel elaboration and optical features of Eu3+-doped CdS nanocrystals in $SiO_2$. Mater Sci Forum 555:389–393
87. Kamalov VF, Little R, Logunov SL, El-Sayed MA (1996) Picosecond electronic relaxation in CdS/HgS/CdS quantum dot quantum well semiconductor nanoparticles. J Phys Chem 100: 6381–6384
88. Kanatzia A, Papageorgiou CH, Lioutas CH, Kyratsi TH (2013) Design of ball-milling experiments on Bi2Te3 thermoelectric material. J Electron Mater 42(7):1652–1660
89. Kang B, Chang SQ, Dai YD, Chen D (2008a) Synthesis of green CdSe/chitosan QDs using a polymer-assisted c-radiation route. Rad Phys Chem 77(7):859–863
90. Kang SH, Bozhilov KN, Myung NV, Mulchandani A, Chen W (2008b) Microbial synthesis of CdS NCs in genetically engineered *E. coli*. Angew Chem Int Ed 47(28):5186–5189. https://doi.org/10.1002/anie.200705806
91. Karimi JA, Mohsenzadeh S (2012) Phytosynthesis of cadmium oxide NPs from Achillea wilhelmsii flowers. J Chem 2013:147613
92. Karkas MD, Porco JA Jr, Stephenson CRJ (2016) Photochemical approaches to complex chemotypes: applications in natural product synthesis. Chem Rev 116(17):9683–9747
93. Kashinath L, Namratha K, Srikantaswamy S, Vinu A, Byrappa K (2017) Microwave treated sol–gel synthesis and characterization of hybrid ZnS–RGO composites for efficient photodegradation of dyes. New J Chem 41:1723–1735
94. Khafajeh R, Molaei M, Karimipour M (2017) Synthesis of ZnSe and ZnSe:Cu quantum dots by a room temperature photochemical (UV-assisted) approach using $Na_2SeO_3$ as Se source and investigating optical properties. Luminescence 32(4):581–587
95. Kharissova OV, Kharisov BI, González CMO, Méndez YP, López I (2019) Greener synthesis of chemical compounds and materials. R Soc Open Sci 6:191378

96. Khiew PS, Huang NM, Radiman S, Ahmad MS (2004) Synthesis and characterization of conducting polyaniline-coated cadmium sulphide nanocomposites in reverse microemulsion. Mater Lett 58(3):516–521
97. Koch CC (1997) Synthesis of nanostructured materials by mechanical milling: problems and opportunities. Nanostruct Mater 9:13–22
98. Koch CC (1991) Mechanical milling and alloying. In: Cahn RW, Haasen P, Kramer EJ (eds) Materials science and technology, vol 15. VCH Verlagsgesellschaft GmbH, Weinheim, pp 193–245
99. Komarneni S, Sakka S, Phule PP, Laine RM (eds) (1998) Sol-gel synthesis and Processisng, Ceramic transactions, vol 95. Wiley, New York
100. Korotcenkov G (2020) Handbook of humidity measurement: methods, materials and technologies, Sensing Materials and Technologies, vol 3. CRC Press, Boca Raton
101. Korotcenkov G (ed) (2010) Chemical sensors: fundamentals of sensing materials. Vol. 1: General approaches. Momentum Press, New York
102. Kowshik M, Deshmukh N, Vogel W, Urban J, Kulkarni SK, Paknikar KM (2002) Microbial synthesis of semiconductor CdS NPs, their characterization, and their use in the fabrication of an ideal diode. Biotechnol Bioeng 78(5):583–588
103. Kristl M, Ban I, Gyergyek S (2013) Preparation of nanosized copper and cadmium chalcogenides by mechanochemical synthesis. Mater Manufact Proces 28(9):1009–1013
104. Kristl M, Ban I, Danč A, Danč V, Drofenik M (2010) A sonochemical method for the preparation of cadmium sulfide and cadmium selenide NPs in aqueous solutions. Ultrason Sonochem 17(5):916–922
105. Kumar SA, Ansary AA, Ahmad A, Khan MI (2007) Extracellular biosynthesis of CdSe QDs by the fungus, Fusarium oxysporum. J Biomed Nanotechnol 3(2):190–194
106. Kumaresan R, Ichimura M, Arai E (2002) Photochemical deposition of ZnSe polycrystalline thin films and their characterization. Thin Solid Films 414:25–30
107. Lagashettya A, Havanoor V, Basavaraja S, Balaji SD, Venkataraman A (2007) Microwave-assisted route for synthesis of nanosized metal oxides. Sci Technol Adv Mater 8:484–493
108. Lamer VK, Dinegar RH (1950) Theory, production and mechanism of formation of monodispersed hydrosols. J Am Chem Soc 72:4847–4854
109. Li J, Wu Q, Wu J (2016) Synthesis of nanoparticles via solvothermal and hydrothermal methods. In: Aliofkhazraei M (ed) Handbook of nanoparticles. Springer, New York, pp 295–328
110. Li H, Wang C, Peng Z, Fu X (2015) A review on the synthesis methods of CdSeS-based nanostructures. J Nanomater 2015:519385
111. Li D, Wang S, Wang J, Zhang X, Liu S (2013) Synthesis of CdTe/TiO2 nanoparticles and their photocatalytic activity. Mater Res Bull 48(10):4283–4286
112. Li H, Qu F (2007) Synthesis of CdTe quantum dots in sol-gel-derived composite silica spheres coated with calix[4]arene as luminescent probes for pesticides. Chem Mater 19:4148–4154
113. Li X-H, Li J-X, Li G-D, Liu D-P, Chen J-S (2007) Controlled synthesis, growth mechanism, and properties of monodisperse CdS colloidal spheres. Eur J Chem A 13:8754–8761
114. Li Z, Hou B, Xu Y, Wu D, Sun Y, Hu W et al (2005) Comparative study of sol–gel-hydrothermal and sol–gel synthesis of titania–silica composite nanoparticles. J Solid State Chem 178(5):1395–1405
115. Li C, Murase N (2004) Synthesis of highly luminescent glasses incorporating CdTe NCs through Sol–Gel processing. Langmuir 20(1):1–4
116. Li Z, Zhang J, Du J, Mu T, Liu Z, Chen J et al (2004) Preparation of cadmium sulfide/poly (methyl methacrylate) composites by precipitation with compressed $CO_2$. J Appl Polym Sci 94(4):1643–1648
117. Li Y, Ding Y, Wang Z (1999) A novel chemical route to ZnTe semiconductor nanorods. Adv Mater 11:847–850
118. Li G, Nogami M (1994) Preparation and optical properties of solgel derived ZnSe crystallites doped in glass films. J Appl Phys 75:4276

119. Liao X-H, Zhu J-J, Chen H-J (2001) Microwave synthesis of nanocrystalline metal sulfides in formaldehyde solution. Mater Sci Eng B 85:85–91
120. Lifshitz E, Dag I, Litvin I, Hodes G, Gorer S, Reisfeld R et al (1998) Optical properties of CdSe nanoparticle films prepared by chemical deposition and sol–gel methods. Chem Phys Lett 288:188–196
121. Liu M, Zhao H, Chen S, Wang H, Quan X (2012) Photochemical synthesis of highly fluorescent CdTe quantum dots for "on–off–on" detection of Cu(II) ions. Inorg Chim Acta 392:236–240
122. Lee HL, Issam AM, Belmahi M, Assouar MB, Rinnert H, Alnot M (2009) Synthesis and characterizations of bare CdS nanocrystals using chemical precipitation method for photoluminescence application. J Nanomater 2009:914501
123. Liu J, Xue D (2010) Morphology-controlled synthesis of CdSe semiconductor through a low-temperature hydrothermal method. Phys Scr T139:014075
124. Liu P, Wang Q, Li X (2009) Studies on CdSe/L-cysteine quantum dots synthesized in aqueous solution for biological labelling. J Phys Chem C 113:7670–7676
125. Loudhaief N, Labiadh H, Hannachi E, Zouaoui M, Ben SM (2018) Synthesis of CdS nanoparticles by hydrothermal method and their effects on the electrical properties of bi-based superconductors. J Superconduct Novel Magnet 31:2305–2312
126. Majid A, Bibi M (2018) Cadmium based II-VI semiconducting nanomaterials. Springer Nature, Cham
127. Majid A, Arshad H, Murtaza S (2015) Synthesis and characterization of Cr doped CdSe NPs. Superlatt Microstr 85:620–623
128. Mal J, Nancharaiah YV, van Hullebusch ED, Lens PNL (2016) Metal chalcogenide quantum dots: biotechnological synthesis and applications. RSC Adv 6:41477–41495
129. Malik MA, Wani MY, Hashim MA (2012) Microemulsion method: a novel route to synthesize organic and inorganic nanomaterials: 1st nano update. Arab J Chem 5(4):397–417
130. Mao Y, Park T-J, Zhang F, Zhou H, Wong SS (2007) Environmentally friendly methodologies of nanostructure synthesis. Small 3(7):1122–1139
131. Menezes FD, Galembeck A, Junior SA (2011) New methodology for obtaining CdTe QDs by using ultrasound. Ultrason Sonochem 18(5):1008–1011
132. Meng L-Y, Wang B, Ma M-G, Lin K-L (2016) The progress of microwave-assisted hydrothermal method in the synthesis of functional nanomaterials. Mater Today Chem 1–2:63–83
133. Mittal AK, Kaler A, Banerjee UC (2012) Free radical scavenging and antioxidant activity of silver NPs synthesized from flower extract of rhododendron dauricum. Nano Biomed Eng 4(3):118–124
134. Mirzaei A, Neri G (2016) Microwave-assisted synthesis of metal oxide nanostructures for gas sensing application. A review Sens Actuators B 237:749–775
135. Mo X, Wang CY, You M, Zhu YR, Chen ZY, Hu Y (2001) A novel ultraviolet-irradiation route to CdS nanocrystallites with different morphologies. Mater Res Bull 36:2277–2282
136. Modeshia DR, Walton RI (2010) Solvothermal synthesis of perovskites and pyrochlores: crystallization of functional oxides under mild conditions. Chem Soc Rev 39:4303–4325
137. Moon J-W, Ivanov IN, Duty CE, Love LJ, Rondinone AJ, Wang W et al (2013) Scalable economic extracellular synthesis of CdS nanostructured particles by a non-pathogenic thermophile. J Industr Microbiol Biotechnol 40:1263–1271
138. Motshekga SC, Pillai SK, Ray SS, Jalama K, Krause RWM (2012) Recent trends in the microwave-assisted synthesis of metal oxide nanoparticles supported on carbon nanotubes and their applications. J Nanomater 2:1–12
139. Mntungwa N, Puilabhotla VSR, Revaprasadu N (2012) The synthesis of core-shell metal-semiconductor nanomaterials. Mater Lett 81:108–111
140. Munirah KMS, Aziz A, Rahman SA, Khan ZR (2013) Spectroscopic studies of sol–gel grown CdS nanocrystalline thin films for optoelectronic devices. Mater Sci Semicond Proc 16:1894–1898

141. Murray CB, Norris DJ, Bawendi MG (1993) Synthesis and characterization of nearly monodisperse CdE (E = sulfur, selenium, tellurium) semiconductor nanocrystallites. J Am Chem Soc 115:8706–8715
142. Muruganandam S, Anbalagan G, Murugadoss G (2017) Structural, electrochemical and magnetic properties of codoped (Cu, Mn) CdS NPs with surfactant PVP. Opt-Intern J Light Electron Opt 131:826–837
143. Niederberger M (2007) Nonaqueous sol-gel routes to metal oxide nanoparticles. Acc Chem Res 40:793–800
144. Nishimura H, Lin Y, Hizume M, Taniguchi T, Shigekawa N, Takagi T et al (2019) Hydrothermal synthesis of ZnSe:Mn quantum dots and their optical properties. AIP Adv 9:025223
145. Nogami M, Nagasaka K, Suzuki T (1992) Sol-gel synthesis of cadmium telluride-microcrystal-doped silica glasses. J Am Ceram Soc 75(1):220–223
146. Nogi K, Hosokawa M, Naito M, Yokoyama T (eds) (2012) Nanoparticle technology handbook. Elsevier, Oxford
147. Omran BA, Whitehead KA, Baek K-H (2021) One-pot bioinspired synthesis of fluorescent metal chalcogenide and carbon quantum dots: applications and potential biotoxicity. Colloid Surf Biointerfaces 200:111578
148. Onwudiwe DC, Krüger TP, Oluwatobi OS, Strydom CA (2014) Nanosecond laser irradiation synthesis of CdS NPs in a PVA system. Appl Surf Sci 290:18–26
149. Ouyang JY, Vincent M, Kingston D, Descours P, Boivineau T, Zaman B et al (2009) Noninjection, onepot synthesis of photoluminescent colloidal homogeneously alloyed CdSeS quantum dots. J Phys Chem C 113(13):5193–5200
150. Qian H, Li L, Ren J (2005) One-step and rapid synthesis of high quality alloyed QDs (CdSe–CdS) in aqueous phase by microwave irradiation with controllable temperature. Mater Res Bull 40(10):1726–1736
151. Panda AB, Glaspell G, El-Shall MS (2006) Microwave synthesis of highly aligned ultranarrow semiconductor rods and wires. J Am Chem Soc 128:2790–2791
152. Pandian SRK, Deepak V, Kalishwaralal K, Gurunathan S (2011) Biologically synthesized fluorescent CdS NPs encapsulated by PHB. Enzym Microb Technol 48(4):319–325
153. Park J, Joo J, Kwon SG, Jang Y, Hyeon T (2007) Synthesis of monodisperse spherical nanocrystals. Angew Chem Intern Ed 46:4630–4660
154. Peng X, Sclamp MC, Kadavanich AV, Alivisatos AP, Epitaxial AP (1997) Growth of highly luminescent CdSe/CdS core/shell nanocrystals with photostability and electronic accessibility. J Am Chem Soc 119:7019–7029
155. Phuruangrat A, Thongtem T, Sinaim H, Thongtem S (2013) Synthesis of cadmium selenide nanorods by polyethylene glycol-assisted solvothermal process. J Experimen Nanosci 8(6): 654–660
156. Plaza DO, Gallardo C, Straub YD, Bravo D, Pérez-Donoso JM (2016) Biological synthesis of fluorescent NPs by cadmium and tellurite resistant Antarctic bacteria: exploring novel natural nanofactories. Microb Cell Factor 15(1):76
157. Rabinal MHK, Gunnagol RM, Hodlur RM (2016) Recent developments in the green syntheses of chalcogenide based semi-conductor nanoparticles. Curr Nanomater 1:12–60
158. Raj FM, Rajendran AJ (2015) Synthesis and characterization of cadmium sulfide NPs for the applications of dye sensitized solar cell. Intern J Innov Res Sci Eng Technol 4(1):56–60
159. Rao BS, Kumar BR, Reddy VR, Rao TS, Chalapathi GV (2011) Preparation and characterization of CdS NPs by chemical co-precipitation technique. Chalcogenide Lett 8(3):177–185
160. Rathinama I, Parvathi AA, Pandiarajan J, Jeyakumaran N, Prithivikumaran N (2013) Influence of annealing temperature on structural and optical properties of CdS thin films prepared by sol-gel spin coating method. In: Proceedings of the "International Conference on Advanced Nanomaterials & Emerging Engineering Technologies" (ICANMEET-20J3), Chennai, India, 24–26 July, 2013, pp 713–717

161. Reddy CV, Vattikuti SP, Shim J (2016) Synthesis, structural and optical properties of CdS NPs with enhanced photocatalytic activities by photodegradation of organic dye molecules. J Mater Sci Mater Electron 27(8):7799–7808
162. Roberts BA, Strauss CR (2005) Toward rapid "green" predictable microwave-assisted synthesis. Acc Chem Res 38:653–661
163. Salavati-Niasari M, Bazarganipour M, Ghasemi-Kooch M (2015) Facile sonochemical synthesis and characterization of CdTe NPs. Synth React Inorg Metal-Org Nano-Metal Chem 45(10):1558–1564
164. Sangsefidi FS, Salavati-Niasari M, Esmaeili-Zare M (2013) Hydrothermal method for synthesis of HgTe nanorods in presence of a novel precursor. Supperlatt Microstructur 62:1–11
165. Saraji, M., Dizajib, H. R., Fallaha, M. (2012). An efficient method for synthesis and characterization of CdS and CdS:Cu NPs by microwave irradiation. In: Proceedings of the 4th international conference on nanostructures, pp. 1495–1497
166. Saravanan L, Pandurangan A, Jayavel R (2012) Synthesis and luminescence enhancement of cerium doped CdS NPs. Mater Lett 66(1):343–345
167. Saravanan P, Gopalan R, Chandrasekaran V (2008) Synthesis and characterisation of nanomaterials. Defence Sci J 58(4):504–516
168. Schanche JS (2003) Microwave synthesis solutions from personal chemistry. Mol Divers 7: 293–300
169. Schneider R, Balan L (2012) Hydrothermal routes for the synthesis of CdSe Core quantum dots. In: Al-Ahmadi A (ed) Nanotechnology and nanomaterials: state of the art of quantum dot systems fabrications. Intech, pp 119–140
170. Schwartz RW, Schneller T, Waser R (2004) Chemical solution deposition of electronic oxide films. C R Chim 7:433–461
171. Serrano T, Gómez I, Colás R, Cavazos J (2009) Synthesis of CdS NCs stabilized with sodium citrate. Colloids Surf A: Physicochem Eng Aspects 338(1):20–24
172. Shafiee S, Akhavan O, Hatami H, Hoseinkhani P (2015) Sol-gel synthesis of thermoluminescent Cd-doped ZnTe nanoparticles. Indian J Pure Appl Phys 53:804–807
173. Shah M, Fawcett D, Sharma S, Tripathy SK, Poinern GEJ (2015) Green synthesis of metallic NPs via biological entities. Materials 8(11):7278–7308
174. Sharma K, Kumar A (2014) Synthesis and characterization of pure and Zn doped CdSe NPs by ultrasonication technique. Am Intern J Res Sci Technol Eng Math 8:75–79
175. Shao M, Xu F, Peng Y, Wu J, Li Q, Zhang S et al (2002) Microwave-templated synthesis of CdS NTs in aqueous solution at room temperature. New J Chem 26(10):1440–1442
176. Sheldrick WS, Wachhold M (1997) Solventothermal synthesis of solid-state chalcogenidometalates. Angew Chem Int Ed Engl 36:206–224
177. Shen L, Bao N, Prevelige PE, Gupta A (2010) *Escherichia coli* bacteria-templated synthesis of nanoporous cadmium sulfide hollow microrods for efficient photocatalytic hydrogen production. J Phys Chem C 114(6):2551–2559
178. Shkir M, Aarya S, Singh R, Arora M, Bhagavannarayana G, Senguttuvan TD (2012) Synthesis of ZnTe nanoparticles by microwave irradiation technique, and their characterization. Nanosci Nanotechnol Lett 4:405–408
179. Singh P, Kim YJ, Wang C, Mathiyalagan R, El-Agamy Farh M, Yang DC (2016) Biogenic silver and gold NPs synthesized using red ginseng root extract, and their applications. Artif Cells Nanomed Biotechnol 44(3):811–816
180. Singh P, Kim YJ, Zhang D, Yang DC (2016) Biological synthesis of NPs from plants and microorganisms. Trends Biotechnol 34(7):588–599
181. Singh BR, Dwivedi S, Al-Khedhairy AA, Musarrat J (2011) Synthesis of stable cadmium sulfide NPs using surfactin produced by *Bacillus amyloliquefaciens* strain KSU-109. Colloids Surf B: Biointerfaces 85(2):207–213
182. Skubi KL, Blum TR, Yoon TP (2016) Dual catalysis strategies in photochemical synthesis. Chem Rev 116(17):10035–10074

183. Sofronov DS, Sofronova EM, Starikov VV, Baumer VN, Matejchenko PV, Galkin SN et al (2013) Microwave synthesis of ZnSe. J Mater Eng Perform 22:1637–1641
184. Solans C, Izquierdo P, Nolla J, Azemar N, Garcia-Celma MJ (2005) Nanoemulsions. Curr Opin Colloid Interface Sci 10:102–110
185. Song J, Dai Z, Guo W, Li Y, Wang W, Li N et al (2013) Preparation of CdTe/CdS/$SiO_2$ core/multishell structured composite NPs. J Nanosci Nanotechnol 13(10):6924–6927
186. Sonker RK, Yadav BC, Gupta V, Tomar M (2020) Synthesis of CdS nanoparticle by sol-gel method as low temperature $NO_2$ sensor. Mater Chem Phys 239:121975
187. Sostaric JZ, Caruso-Hobson RA, Mulvaney P, Grieser F (1997) Ultrasound-induced formation and dissolution of colloidal CdS. J Chem Soc Faraday Trans 93(9):1791–1795
188. Starnic V, Etsell TH, Pierre AC, Mikula RJ (1997) Sol-gel processing of ZnS. Mater Lett 31: 35–38
189. Suriwong T, Phuruangrat A, Thongtem S, Thongtem T (2015) Synthesis, characterization and photoluminescence properties of CdTe nanocrystals. J Ovonic Res 11(6):257–261
190. Suslick KS, Fang MM, Hyeon T, Mdleleni MM (1999) Applications of sonochemistry to materials synthesis. In: Crum LA, Mason TJ, Reisse JL, Suslick KS (eds) Sonochemistry and Sonoluminescence. Springer, Netherlands, pp 291–320
191. Sweeney RY, Mao C, Gao X, Burt JL, Belcher AM, Georgiou G et al (2004) Bacterial biosynthesis of cadmium sulfide NCs. Chem Biol 11(11):1553–1559
192. Tan GL, Yu XF (2009) Capping the ball-milled CdSe nanocrystals for light excitation. J Phys Chem C 113(20):8724–8729
193. Tan GL, Zhang L, Yu XF (2009) Preparation and optical properties of CdS NCs prepared by a mechanical alloying process. J Phys Chem C 114(1):290–293
194. Tan GL, Hömmerich U, Temple D, Wu NQ, Zheng JG, Loutts G (2003) Synthesis and optical characterization of CdTe NCs prepared by ball milling process. Scripta Mater 48(10): 1469–1474
195. Taurino AM, Epifani M, Taccoli T, Iannotta S, Siciliano P (2003) Innovative aspects in thin film technologies for nanostructured materials in gas sensor devices. Thin Solid Films 436:52–63
196. Tho NTM, An TNM, Tri MD, Sreekanth TVM, Lee JS, Nagajyothi PC et al (2013) Green synthesis of silver NPs using Nelumbo nucifera seed extract and its antibacterial activity. Acta Chim Slovenica 60(3):673–678
197. Tolia JV, Chakraborty M, Murthy ZVP (2012) Mechanochemical synthesis and characterization of group II-VI semiconductor NPs. Partic Sci Technol 30(6):533–542
198. Tsuzuki T, McCormick PG (1997) Synthesis of CdS QDs by mechanochemical reaction. Appl Phys A: Mater Sci Proces 65(6):607–609
199. Ulloa G, Collao B, Araneda M, Escobar B, Álvarez S, Bravo D et al (2016) Use of acidophilic bacteria of the genus Acidithiobacillus to biosynthesize CdS fluorescent nanoparticles (quantum dots) with high tolerance to acidic pH. Enzyme Microbiol Technol 95:217–224
200. Vaquero F, Navarro RM, Fierro JLG (2017) Influence of the solvent on the structure, morphology and performance for H2 evolution of CdS photocatalysts prepared by solvothermal method. Appl Catal B Environ 203:753–767
201. Venci X, Gerge A, Raj AD, Irudayaraj AA, Raj DMA, Jayakumar G, Sundaram SJ (2021) Tuning the morphology and band gap of CdSe nanoparticles via solvothermal method. Mater Today 36(2):459–463
202. Veeranarayanan S, Poulose AC, Mohamed MS, Nagaoka Y, Iwai S, Nakagame Y et al (2012) Synthesis and application of luminescent single CdS quantum dot encapsulated silica NPs directed for precision optical bioimaging. Intern J Nanomed 7:3769
203. Wan B, Hu C, Feng B, Xu J, Zhang Y, Tian Y (2010) Optical properties of ZnTe nanorods synthesized via a facile low-temperature solvothermal route. Mater Sci Eng B 171:11–15
204. Wang J, Liu S, Mu Y, Liu L, Runa A, Su P et al (2017) Synthesis of uniform cadmium sulphide thin film by the homogeneous precipitation method on cadmium telluride nanorods

and its application in three-dimensional heterojunction flexible solar cells. J Colloid Interface Sci 505:59–66
205. Wang Q, Li J, Bai Y, Lian J, Huang H, Li Z et al (2014) Photochemical preparation of Cd/CdS photocatalysts and their efficient photocatalytic hydrogen production under visible light irradiation. Green Chem 16(5):2728–2735
206. Wang Q, Pan D, Jiang S, Ji X, An L, Jiang B (2006) A solvothermal route to size- and shape-controlled CdSe and CdTe nanocrystals. J Crystal Growth 286:83–90
207. Wang GZ, Chen W, Liang CH, Wang YW, Meng GW, Zhang LD (2001) Preparation and characterization of CdS nanoparticles by ultrasonic irradiation. Inorg Chem Commun 4(4): 208–210
208. Wang H, Zhang J-R, Zhu J-J (2001b) A microwave assisted heating method for the rapid synthesis of sphalrite-type mercury sulfide nanocrystals with different sizes. J Cryst Growth 233:829–836
209. Wang CY, Mo X, Zhou Y, Zhu YR, Liu HT, Chen ZY (2000) A convenient ultraviolet irradiation technique for in situ synthesis of CdS nanocrystallites at room temperature. J Mater Chem 10:607–608
210. Whiffen RK, Montone A, Pietrelli L, Pilloni L (2021) On tailoring co-precipitation synthesis to maximize production yield of nanocrystalline wurtzite ZnS. Nano 11:715
211. Yadav S, Yashas SR, Shivaraju HP (2021) Transitional metal chalcogenide nanostructures for remediation and energy: a review. Environ Chem Lett 19:683–3700
212. Yan YL, Li Y, Qian XF, Yin J, Zhu ZK (2003) Preparation and characterization of CdSe NCs via $Na_2SO_3$-assisted photochemical route. Mater Sci Eng B 103(2):202–206
213. Yang G, Park S-J (2019) Conventional and microwave hydrothermal synthesis and application of functional materials: a review. Materials 12:1177
214. Yang Y, Gao MY (2005) Preparation of fluorescent $SiO_2$ particles with single CdTe nanocrystal cores by the reverse microemulsion method. Adv Mater 17(19):2354–2357
215. Yang H, McCormick PG (1998) Mechanically activated reduction of nickel oxide with graphite. Metall Mater Trans B Process Metall Mater Process Sci 29:449–455
216. Yu S-H (2001) Hydrothermal/solvothermal processing of advanced ceramic materials. J Ceram Soc Jpn 109(5):S65–S75
217. Yu SH, Wu YS, Yang J, Han ZH, Xie Y, Qian YT, Liu XM (1998) A novel solventothermal synthetic route to nanocrystalline CdE (E = S, Se, Te) and morphological control. Chem Mater 10:2309–2312
218. Yu SH, Shu L, Wu YS, Tang KB, Xie Y, Qian YT, Zhang YH (1998) Benzene-thermal synthesis and optical properties of CdS nanocrystalline. Nanostruct Mater 10:1307–1316
219. Xi LF, Lam YM (2007) Synthesis and characterization of CdSe NRs using a novel microemulsion method at moderate temperature. J Colloid Interface Sci 316(2):771–778
220. Xiong C, Liu M, Zhu X, Tang A (2019) A general one-pot approach to synthesize binary and ternary metal sulfide nanocrystals. Nanoscale Res Lett 14:19
221. Xu H, Zeiger BW, Suslick KS (2013) Sonochemical synthesis of nanomaterials. Chem Soc Rev 42(7):2555–2567
222. Zelner M, Minti H, Reisfeld R, Cohen H, Feldman Y, Cohen SR, Tenne R (2001) Preparation and characterization of CdTe nanoparticles in zirconia films prepared by the sol gel method. J Sol-Gel Sci Technol 20:153–160
223. Zhan HJ, Zhou PJ, Ma R, Liu XJ, He YN, Zhou CY (2014) Enhanced oxidation stability of quasi core-shell alloyed CdSeS QDs prepared through aqueous microwave synthesis technique. J Fluoresc 24(1):57–65
224. Zhang R, Li G, Zhang Y (2017) Photochemical synthesis of CdS-MIL-125 (Ti) with enhanced visible light photocatalytic performance for the selective oxidation of benzyl alcohol to benzaldehyde. Photochem Photobiol Sci 16(6):996–1002
225. Zhang YC, Wang GY, Hu XY, Shi QF, Qiao T, Yang Y (2005) Phase-controlled synthesis of ZnS nanocrystallites by mild solvothermal decomposition of an air-stable single-source molecular precursor. J Crystal Growth 284:554–560

226. Zhang Q, Huang F, Li Y (2005) Cadmium sulfide NRs formed in microemulsions. Colloids Surf A Physicochem Eng Asp 257:497–501
227. Zhang Y, Li Y (2004) Synthesis and characterization of monodisperse doped ZnS nanospheres with enhanced thermal stability. J Phys Chem B 108:17805
228. Zhang H, Wang L, Xiong H, Hu L, Yang B, Li W (2003) Hydrothermal synthesis for high-quality CdTe nanocrystals. Adv Mater 15:1712
229. Zhao WB, Zhu JJ, Chen HY (2003) Photochemical preparation of rectangular PbSe and CdSe NPs. J Crystal Growth 252(4):587–592
230. Zhong B, Kang W, Zhang Z, Zhang L, Ma B (2020) Facile one-pot solvothermal synthesis of CdTe nanorods and their photoelectrical properties. CrystEngComm 22:3927–3393
231. Zhong WH (2012) Nanoscience and nanomaterials: synthesis, Manufacturing and Industry Impacts. DEStech Publications, Inc, Lancaster
232. Zhong H, Mirkovic T, Scholes GD (2011) Nanocrystal synthesis. In: Andrews DL, Scholes GD, Wiederrecht GP (eds) Comprehensive nanoscience and technology, vol 5. Elsevier, New York, pp 153–201
233. Zhou GJ, Li SH, Zhang YC, Fu YZ (2014) Biosynthesis of CdS NPs in banana peel extract. J Nanosci Nanotechnol 14(6):4437–4442
234. Zhou SM, Feng YS, Zhang LD (2003) Sonochemical synthesis of large-scale single crystal CdS NRs. Mater Lett 57(19):2936–2939
235. Zhu J-J, Wang H (2004) Synthesis of metal chalcogenide nanoparticles synthesis of metal chalcogenide nanoparticles. In: Nalwa HS (ed) Encyclopedia of nanoscience and nanotechnology, vol 10. American Scientific Publishers, pp 347–367
236. Zhu J, Liao X, Zhao X, Wang J (2001) Photochemical synthesis and characterization of CdSe NPs. Mater Lett 47(6):339–343
237. Zhu J, Koltypin Y, Gedanken A (2000) General sonochemical method for the preparation of nanophasic selenides: synthesis of ZnSe nanoparticles. Chem Mater 12:73–78
238. Zhu J, Liu S, Palchik O, Koltypin Y, Gedanken A (2000) A novel sonochemical method for the preparation of nanophasic sulfides: synthesis of HgS and PbS nanoparticles. J Solid State Chem 153:342–350
239. Zhu J, Palchik O, Chen S, Gedanken A (2000) Microwave assisted preparation of CdSe, PbSe, and $Cu_{2-x}Se$ NPs. J Phys Chem B 104(31):7344–7347
240. Ziegler J, Merkulov A, Grabolle M, Resch-Genger U, Nann T (2007) High-quality ZnS shells for CdSe nanoparticles: rapid microwave synthesis. Langmuir 23:7751–7759
241. Zou Y, Li DS, Yang D (2010) Noninjection synthesis of CdS and alloyed $CdS_xSe_{1-x}$ nanocrystals without nucleation initiators. Nanoscale Res Lett 5(6):966–971
242. Zuala L, Agarwal P (2020) Growth and characterization of ZnSe nanocrystals synthesized using solvothermal process. J Mater Sci Mater Electron 31:14756–14766